Journal Pre-proof

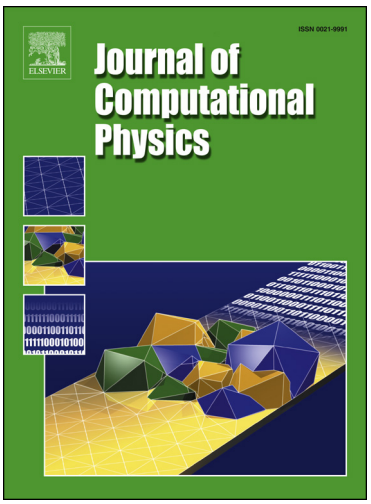

Kinetic-energy- and pressure-equilibrium-preserving schemes for real-gas turbulence in the transcritical regime

Marc Bernades, Lluís Jofre and Francesco Capuano

PII: S0021-9991(23)00572-7
DOI: https://doi.org/10.1016/j.jcp.2023.112477
Reference: YJCPH 112477

To appear in: *Journal of Computational Physics*

Received date: 30 March 2023
Revised date: 22 August 2023
Accepted date: 30 August 2023

Please cite this article as: M. Bernades, L. Jofre and F. Capuano, Kinetic-energy- and pressure-equilibrium-preserving schemes for real-gas turbulence in the transcritical regime, *Journal of Computational Physics*, 112477, doi: https://doi.org/10.1016/j.jcp.2023.112477.

Highlights

- Development of a framework to derive kinetic-energy- and pressure-equilibrium-preserving schemes for discontinuity-free, real-gas compressible flows.
- Conditions to obtain pressure-equilibrium for linear finite-differencing schemes.
- Demonstration of a *barrier* related to the discrete fulfillment of the chain rule.
- Derivation of a novel class of stable and oscillation-free schemes.
- Discrete enforcement of pressure equilibrium is of utmost importance in high-pressure transcritical flows.

Kinetic-energy- and pressure-equilibrium-preserving schemes for real-gas turbulence in the transcritical regime

Marc Bernades[a], Lluís Jofre[a], Francesco Capuano[a,*]

[a]*Department of Fluid Mechanics, Universitat Politècnica de Catalunya · BarcelonaTech (UPC), Barcelona 08034, Spain*

Abstract

Numerical simulations of compressible turbulent flows governed by real-gas equations of state, such as high-pressure transcritical flows, are strongly susceptible to instabilities. In addition to the inherent multi-scale nature of the flow, the presence of a pseudo-interface can generate spurious pressure oscillations when conventional schemes are utilized. This study proposes a general framework to derive and analyze discretization methods that are able to preserve kinetic energy by convection, and simultaneously maintain pressure equilibrium in discontinuity-free compressible real-gas flows. The formal analysis reveals that the discrete pressure-equilibrium condition can be fulfilled at most to second-order accuracy, as it requires the spatial differential operator to satisfy a discrete chain rule when total, or internal energy, are directly discretized. A novel class of schemes based on the solution of a pressure equation is thus proposed, which preserves mass, momentum, kinetic energy and pressure equilibrium, but not total energy. Extensive numerical tests of increasing complexity confirm the theoretical predictions, and show that the proposed scheme is capable of providing non-dissipative, stable and oscillation-free simulations, unlike existing methods tailored for the transcritical regime.

Keywords: Kinetic-energy-preserving schemes, Pressure-equilibrium-preserving schemes, Total energy conservation, High-pressure, Supercritical fluids, Turbulence

1. Introduction

Supercritical fluids are substances operating at temperatures and pressures above their critical values (T_c, P_c), where no clear phase separation is present. However, within this region, they can be distinguished between: (i) supercritical fluids with gas-like density and transport coefficients, and (ii) liquid-like fluids with a large density, and transport coefficients similar to those of a liquid [1]. In so-called *transcritical* conditions, flows operate in virtually multi-phase conditions, i.e., there is coexistence of both gas-like and liquid-like states. However, unlike subcritical two-phase flow, single-component transcritical flows are always in the continuous regime, as a consequence of the small Knudsen numbers ($Kn \ll 1$) resulting from small mean free paths at high pressures [2, 3]. Trans- and supercritical fluids are relevant in many engineering applications, including internal-combustion and rocket engines, among others. Furthermore, the peculiar thermophysical characteristics described above can be fine-tuned for several purposes. For instance, they can be leveraged to achieve turbulent regimes in microfluidic devices [4], a concept of remarkable interest for energy applications given the enhanced mixing and transfer rates of turbulent flows [5, 6].

High-fidelity numerical simulations can be an invaluable tool to elucidate the underlying physics of trans- and supercritical fluids turbulence and to conduct application-oriented *in-silico* experiments, especially in light of the difficulties associated with *in-vitro* characterizations of this regime. Nonetheless, they come with remarkable challenges. The inherent broadband nature of the flow at sufficiently high Reynolds numbers

*Corresponding Author
Email address: francesco.capuano@upc.edu (Francesco Capuano)

requires methods with minimum dissipation and dispersion errors, in order to capture the vast range of time/length scales and to correctly represent the inter-scale energy transfer. However, a straightforward implementation of non-dissipative central schemes is known to promote unbounded amplification of aliasing errors through non-linear interactions, especially on marginally-resolved grids [7, 8]. Furthermore, failure of maintaining pressure equilibrium at the (pseudo-)interface between liquid-like and gas-like phases can result in spurious pressure oscillations, a phenomenon also observed when simulating material interfaces in ideal-gas multi-component flow problems [9], or even in single-component conditions [10]. For supercritical regimes governed by real-gas equations of state, the situation is further exacerbated by the fact that thermodynamic relations can become strongly non-linear, especially across the pseudo-boiling region. This can intensify the amplitude of the pressure oscillations and even lead to solution divergence [11]. Therefore, numerical methods for trans-/supercritical fluids turbulence should ideally be:

1. free of numerical and artificial dissipation[1];
2. free of spurious pressure oscillations;
3. stable, i.e., non-divergent when run at inviscid conditions.

Several numerical strategies have been developed to deal with supercritical turbulence. Special research efforts have been devoted to prevent the generation of spurious pressure oscillations, an issue that has long hampered the feasibility of scale-resolving simulations of, for instance, transcritical fuel injection. The corresponding approaches can be roughly divided into two classes: (i) double-flux models and (ii) pressure-based approaches. In both cases, the idea is to enforce the pressure equilibrium in the vicinity of the pseudo-phase interface. The double-flux concept was originally proposed by Abgrall and Karni [12] in the context of multi-fluid simulations. In this approach, internal energy is "frozen" within the time-integration step to artificially enforce pressure equilibrium at a material interface. This method has been recently extended to transcritical flows by Ma et al. [13]. In pressure-based approaches [14, 15], an equation for pressure is solved in place of, for example, one for total energy. This permits to have direct control on pressure, and has allowed stable simulations of transcritical flows, although with the addition of artificial dissipation. More recently, Lacaze et al. [16] compared pressure-, enthalpy- and internal-energy-based formulations in terms of stability and pressure behaviour. In all of the above-mentioned works, the discretization was based on the conservative (*divergence*) formulation of the convective terms of the Navier-Stokes equations, which is known to be non-linearly unstable in convection-dominated problems [7]. Stability was therefore achieved using either filtering [17] or hybridization with upwind-biased methods, such as HLLC [18] or WENO schemes [19]. While succeeding in stabilizing the simulations, these approaches have several drawbacks: (i) robustness is achieved at the expense of suppressing part of the turbulent energy spectrum; (ii) it is challenging to distinguish instabilities related to the convective term from those associated with the lack of pressure equilibrium; and (iii) the filtering process can interfere with thermodynamic non-linearities and in turn amplify pressure oscillations [16].

In this work, a novel approach inspired by the paradigm of *physics-compatible* discretizations is proposed and assessed. The idea is to construct numerical schemes that are simultaneously able to enforce: (i) discrete kinetic-energy preservation (KEP) by convection, i.e., ensuring that convective terms do not spuriously contribute to the discrete kinetic energy balance, and (ii) discrete pressure-equilibrium preservation (PEP), i.e., the property of maintaining constant pressure when both pressure and velocity are initially uniform. The literature on KEP methods is now relatively vast. A popular way of enforcing this property is to expand the convective terms in so-called *split* forms. A scheme of this kind was initially proposed by Feiereisen et al. [20], based on a quadratic expansion of the convective terms. This approach has been subsequently extended to cubic splittings by Kennedy and Gruber [21], then recast in a locally-conservative formulation by Pirozzoli [22] and recently generalized to a two-parameter class of KEP split forms [7, 23]; the latter family will constitute the basis for the developments presented in this paper. Recent KEP schemes based on split forms [24, 25] have been designed to also enforce the correct exchange of internal and kinetic energy at

[1]Here a distinction is made between *numerical* dissipation, namely an undesired dissipative-like behaviour of the discretization method employed, and *artificial* dissipation, which is instead deliberately added to stabilize the simulation.

the discrete level [26]. In other notable approaches, square-root variable formulations have been utilized to mimic the skew-symmetry of the convective operators as in incompressible flows [27, 28], or to extend the rotational form to variable-density models [29]. All the above-mentioned KEP schemes have demonstrated excellent robustness with no numerical dissipation, and are therefore considered an essential component for scale-resolving simulations of compressible turbulent flows. On the other hand, the idea of enforcing pressure-equilibrium preservation at a discrete level is relatively recent and has been receiving considerable attention over the past few years. In this regard, PEP schemes have been proposed and analyzed for ideal-gas flows [10, 30], later extended to stiffened-gas thermodynamics [31] and, very recently, to non-reacting multi-component mixtures of calorically-perfect species [32], based again on a carefully-designed split of the convective terms. The extension of this approach to real-gas thermodynamics is challenging due to the non-linear relationship between pressure and internal energy, and is yet to be attempted. It is conjectured that the enforcement of both KEP and PEP can lead to stable and reliable simulations of supercritical turbulence without the need for any form of artificial stabilization. The objectives of this work are therefore twofold: (i) introduce a framework to derive KEP and PEP schemes for discontinuity-free[2] compressible flows governed by a general, real-gas equation of state; and (ii) assess the properties of the resulting schemes and their overall behavior with respect to several state-of-the-art methods. In this regard, the paper is organized as follows. First, in Section 2, the flow physics modeling of supercritical fluids is presented. Next, the discretization frameworks considered in this work are described and numerically analyzed in Section 3. Numerical results are presented in Section 4. Finally, Section 5 reports concluding remarks and future directions.

2. Flow physics modeling

The framework utilized for studying supercritical fluids turbulence in terms of (i) equations of fluid motion, (ii) real-gas thermodynamics and (iii) high-pressure transport coefficients is described below.

2.1. Equations of fluid motion

The turbulent flow motion of supercritical fluids is generally described by the following set of conservation equations of mass, momentum, and total energy

$$\frac{\partial \rho}{\partial t} + \nabla \cdot (\rho \mathbf{u}) = 0, \tag{1a}$$

$$\frac{\partial (\rho \mathbf{u})}{\partial t} + \nabla \cdot (\rho \mathbf{u}\mathbf{u}) = -\nabla P + \nabla \cdot \boldsymbol{\tau}, \tag{1b}$$

$$\frac{\partial (\rho E)}{\partial t} + \nabla \cdot (\rho \mathbf{u} E) = -\nabla \cdot \boldsymbol{q} - \nabla \cdot (P\mathbf{u}) + \nabla \cdot (\boldsymbol{\tau} \cdot \mathbf{u}), \tag{1c}$$

where ρ is the density, $\mathbf{u}$ is the velocity vector, P is the pressure, E is the specific total energy, $\boldsymbol{\tau} = \mu \left(\nabla \mathbf{u} + \nabla \mathbf{u}^T\right) - (2\mu/3)(\nabla \cdot \mathbf{u})\boldsymbol{I}$ is the viscous stress tensor with μ the dynamic viscosity and $\boldsymbol{I}$ the identity matrix, and $\boldsymbol{q} = -\kappa \nabla T$ is the Fourier heat conduction flux with κ the thermal conductivity.

The transport equation for total energy, Eq. (1c), can be equivalently substituted by the evolution equation of another thermodynamic variable using the equation of state and basic rules of calculus. In this work, special emphasis will be placed on pressure. Assuming generically that $P = P(\rho, e)$ and expanding the time derivative of pressure using the chain rule with respect to time leads to

$$\frac{\partial P}{\partial t} = P_\rho \frac{\partial \rho}{\partial t} + P_e \frac{\partial e}{\partial t}, \tag{2}$$

[2] In the present work, all the thermo-fluid-dynamic quantities are considered to be smoothly varying in space, even across (pseudo-)interfaces.

where e is the specific internal energy and

$$P_\rho = \left(\frac{\partial P}{\partial \rho}\right)_e, \quad P_e = \left(\frac{\partial P}{\partial e}\right)_\rho, \tag{3}$$

are the Jacobians of pressure with respect to the state variables ρ and e. This particular choice for the state-variables pair is especially advantageous due to the existence of closed-form expressions for the Jacobians, specifically: $P_e = (1/c_v)\left(\partial P/\partial T\right)_\rho$ and $P_\rho = 1/\left(\rho\beta_s\right) - \left(P/\rho^2\right)P_e$, where $c_v = T\left(\partial s/\partial T\right)_\rho$ is the isochoric specific heat capacity with s the specific entropy, and $\beta_s = -(1/v)\left(\partial v/\partial P\right)_s$ is the isentropic compressibility with $v = 1/\rho$ the specific volume. The analytical expressions for $\left(\partial P/\partial T\right)_\rho$,β_s and c_v within the Peng-Robinson framework are reported in [2]. Upon properly deriving the material derivative of density, momentum and internal energy from Eqs. (1a)-(1c), and using the product rule and the chain rule with respect to space, the pressure evolution equation can be finally written as

$$\frac{\partial P}{\partial t} + \nabla\cdot(P\mathbf{u}) = -\left(\rho c^2 - P\right)\nabla\cdot\mathbf{u} + \frac{1}{\rho}\frac{\beta_v}{c_v\beta_T}(\boldsymbol{\tau}:\nabla\otimes\mathbf{u} - \nabla\cdot\boldsymbol{q}), \tag{4}$$

where $c^2 = 1/(\rho\beta_s) = P_\rho + P/\rho^2 P_e$ is the speed of sound, $\beta_v = (1/v)\left(\partial v/\partial T\right)_P$ is the volume expansivity, and $\beta_T = -(1/v)\left(\partial v/\partial P\right)_T$ is the isothermal compressibility. The system constituted by Eqs. (1a)-(1b) and Eq. (4) is formally equivalent to the one evolving total energy; however, it can lead to different discrete properties, as it will be outlined in Section 3.

2.2. Real-gas thermodynamics

The thermodynamic space of solutions for the state variables pressure P, temperature T, and density ρ of a single substance is described by an equation of state. One popular choice for systems at high pressures, which is used in this study, is the Peng-Robinson equation of state [33] written as

$$P = \frac{R_u T}{\bar{v} - b} - \frac{a}{\bar{v}^2 + 2b\bar{v} - b^2}, \tag{5}$$

with R_u the universal gas constant, $\bar{v} = W/\rho$ the molar volume, and W the molecular weight. The coefficients a and b take into account real-gas effects related to attractive forces and finite packing volume, respectively, and depend on the critical temperature T_c, critical pressure P_c, and acentric factor ω. They are defined as

$$a = 0.457\frac{(\mathrm{R_u}T_c)^2}{P_c}\left[1 + \tilde{c}\left(1 - \sqrt{T/T_c}\right)\right]^2 \quad \text{and} \quad b = 0.078\frac{\mathrm{R_u}T_c}{P_c}, \tag{6}$$

where coefficient $\tilde{c}$ is provided as a function of the acentric factor ω by

$$\tilde{c} = \begin{cases} 0.380 + 1.485\omega - 0.164\omega^2 + 0.017\omega^3 & \text{if } \omega > 0.49, \\ 0.375 + 1.542\omega - 0.270\omega^2 & \text{otherwise.} \end{cases} \tag{7}$$

The Peng-Robinson real-gas equation of state needs to be supplemented with the corresponding high-pressure thermodynamic variables based on departure functions calculated as a difference between two states. In particular, their usefulness is to transform thermodynamic variables from ideal-gas conditions (low pressure - only temperature dependant) to supercritical conditions (high pressure). The ideal-gas parts are calculated by means of the NASA 7-coefficient polynomial [34], while the analytical departure expressions to high pressures are derived from the Peng-Robinson equation of state as detailed in Jofre & Urzay [2].

2.3. High-pressure transport coefficients

The high pressures involved in the analyses conducted in this work prevent the use of simple relations for the calculation of the dynamic viscosity μ and thermal conductivity κ. In this regard, standard methods for computing these coefficients for Newtonian fluids are based on the correlation expressions proposed by Chung *et al.* [35, 36]. These correlation expressions are mainly function of critical temperature T_c and density ρ_c, molecular weight W, acentric factor ω, association factor κ_a and dipole moment $\mathcal{M}$, and the NASA 7-coefficient polynomial [34]; further details can be found in dedicated works, like for example [2, 37].

3. Discretization frameworks

This section describes: (i) a general framework to attain kinetic-energy-preservation (KEP) and pressure-equilibrium-preservation (PEP) schemes for compressible flows governed by a general equation of state, and (ii) existing methods utilized for trans-/supercritical fluids turbulence.

3.1. KEP and PEP schemes

The equations of fluid motion introduced in Section 2.1 are numerically tackled by employing a standard semi-discretization procedure, i.e., they are firstly discretized in space and then integrated in time. Spatial differential operators are treated using centered finite-differencing formulas; a second-order scheme is considered in this paper, although the results can be generalized to formulas of any order that satisfy a discrete summation-by-parts rule (unless otherwise indicated). The discussion will be specifically based on a finite-difference framework; however, the proposed approach also encompasses finite-volume schemes; the reader is referred to, e.g., [38] for details about the relationship between the two formulations. All the flow variables are assumed to be colocated in space. Time derivatives are treated analytically; in practice, temporal errors (in this case associated with Runge-Kutta methods) are assumed to be kept under control by using sufficiently small time steps [39]. Since both KEP and PEP are *inviscid* properties, the Euler equations will be considered in this section; also, for simplicity, but without loss of generality, developments will be presented for the one-dimensional case. Under such hypotheses, the semi-discretized equations read:

$$\rho_t = -C_\rho, \tag{8a}$$

$$(\rho u)_t = -C_{\rho u} - \delta_x P, \tag{8b}$$

$$(\rho E)_t = -\underbrace{(C_{\rho e} + C_{\rho k})}_{C_{\rho E}} - \Pi_{\rho E}, \tag{8c}$$

where subscript t indicates derivation with respect to time, C represents the (semi-discretized) convective terms, and δ_x is the discrete second-order centered derivative operator, which satisfies the summation-by-parts rule but not, e.g., the product rule. The convective term in the total energy equation has been split into convection associated with internal ($C_{\rho e}$) and kinetic energy ($C_{\rho k}$); $\Pi_{\rho E} = \delta_x(Pu)$ is the pressure term. Within this discrete framework, each of the variables in Eqs. (8a)-(8c) is a $N-$sized vector, where N is the number of grid points, and δ_x can be represented as a $N \times N$ derivative matrix. The conservation equations are supplemented by the equation of state, which hereinafter is generically written as $P = P(\rho, e)$.

3.1.1. KEP conditions

Non-dissipative, stable simulations of compressible discontinuity-free turbulent flows have been shown to be achievable by enforcing the KEP property, i.e., ensuring that the discretization of the convective term does not spuriously contribute to the discrete kinetic energy balance. For compressible flow, a family of KEP formulations for the convective term has been recently derived [23], and is briefly summarized here. The underlying idea is to express the convective terms appearing in Eqs. (8a)–(8c) as a linear combination of *split* forms, i.e., all the possible consistent expressions of the derivative of the triple product $\rho u \phi$:

$$C^D_{\rho\phi} = \delta_x \rho u \phi, \tag{9a}$$

$$C^\phi_{\rho\phi} = \phi \delta_x \rho u + \rho u \delta_x \phi, \tag{9b}$$

$$C^u_{\rho\phi} = u \delta_x \rho \phi + \rho \phi \delta_x u, \tag{9c}$$

$$C^\rho_{\rho\phi} = \rho \delta_x u \phi + \phi u \delta_x \rho, \tag{9d}$$

$$C^L_{\rho\phi} = \rho \phi \delta_x u + \rho u \delta_x \phi + \phi u \delta_x \rho, \tag{9e}$$

where ϕ is the transported scalar, e.g., $\phi = 1$ for C_ρ and $\phi = u$ for $C_{\rho u}$. The *generalized* energy is defined as $G^\phi = \rho\phi^2/2$, and it discretely evolves according to $G^\phi_t = \phi(\rho\phi)_t - \phi^2/2\rho_t$; of note, its evolution depends exclusively on the equation-pair constituted by the continuity and the $\rho\phi$-equation. Kinetic energy $\rho k = G^u$

is of particular interest for both physical and stability reasons; upon enforcing discrete conservation of global kinetic energy by convection [23, 38]:

$$\frac{\mathrm{d}}{\mathrm{d}t}\sum_N \rho k = -\underbrace{\sum_N \left[uC_{\rho u} - \frac{u^2}{2}C_\rho\right]}_{=0} - \sum_N u\delta_x P, \tag{10}$$

a two-parameter family of energy-preserving formulations can be found [23]. In particular, the requirement of local conservation of primary invariants (mass, momentum, total energy) leads to the exclusion of $C^L_{\rho\phi}$, which cannot be expressed as a difference of fluxes [23]. As a consequence, a one-parameter family of locally conservative KEP formulations is finally obtained:

$$C^{\mathrm{KEP}}_{\rho\phi} = \xi\frac{C^D_{\rho\phi} + C^\phi_{\rho\phi}}{2} + (1-\xi)\frac{C^u_{\rho\phi} + C^\rho_{\rho\phi}}{2}, \tag{11}$$

where the cases $\xi = 0$, $\xi = 1$ and $\xi = 1/2$ provide the Feiereisen, the "C" form [23] and the so-called Kennedy-Gruber-Pirozzoli (KGP) formulations respectively. For each form of this family, it is possible to define an associated numerical flux based on an arithmetic mean of the flow variables or of their cross-products; see [23] for details[3]. Working directly in a finite-volume framework, other classes of schemes can be obtained that may or may not be recast as a linear combination of finite-difference split forms. For instance, numerical flux functions based on the logarithmic average, or on its generalizations, have been developed to achieve entropy conservation for ideal-gases [40, 41], polytropic models [42], or thermally-perfect gases and multi-component flows [43, 44, 45, 46]. An approach based on a square-root density splitting was recently proposed by Edoh [29], which induces a geometric average in the numerical fluxes. The present study focuses on the family provided by Eq. (11), mostly due to its simplicity, ease of implementation and efficient computational cost, and as a first step towards the analysis of *supra*-conservative discretizations for real-gas thermodynamics [47]. General classes of numerical flux functions with secondary conservation properties will be considered as part of future work.

When Eq. (11) is used for $\phi = 1$ and $\phi = u$, the resulting algorithm preserves mass, momentum and kinetic energy by convection both globally and locally. In particular, the KGP scheme has proved to be particularly robust in previous works, compared to other kinetic-energy-preserving splittings [23]. Any scheme presented in this section is based on the KGP splitting for continuity and momentum. The symbol $C^{\mathrm{KGP}}_{\rho\phi}$ will be used for convective terms expressed in KGP form.

An unspecified degree of freedom remains with regards to the discretization of the convective and pressure terms in the total energy equation. With regards to the pressure term $\Pi_{\rho E}$, as a double product it can be generally discretized as a combination of a *conservative* and an *advective* formulation:

$$\Pi_{\rho E} = \eta\delta_x(Pu) + (1-\eta)(p\delta_x u + u\delta_x P), \tag{12}$$

where η is a free parameter. Alternatively, it can be reformulated as the triple product

$$\Pi_{\rho E} = \delta_x(\rho\hat{p}u), \tag{13}$$

where $\hat{p} = P/\rho$, and therefore all the split forms in Eq. (9) apply. In some previous works [22, 48], the pressure term in Eq. (8c) was expressed as in Eq. (13) and incorporated into convection, and the KGP split was applied to enthalpy (i.e., $\phi = h = e + u^2/2 + \hat{p}$). The scheme obtained by evolving Eqs. (1a)–(1c), with the KGP split applied to all the convective terms and to enthalpy in the total energy equation will be referred hereinafter to as KGP-Et. The application of a KEP scheme to $C_{\rho E}$ leads to preservation of $G^E = \rho E^2$ by convection, which is a quantity with no clear physical meaning. Many other choices are

[3]For instance, the advective formulation C^ρ_ρ admits a numerical flux $F_{i+1/2} = 1/2\,(\rho_{i+1}u_i + \rho_i u_{i+1})$, while the KGP formulation $C^{\mathrm{KGP}}_{\rho\phi}$ corresponds to $F_{i+1/2} = 1/8(\rho_i + \rho_{i+1})(u_i + u_{i+1})(\phi_i + \phi_{i+1})$.

possible and lead to different discrete properties; for instance, the split for $C_{\rho E}$ does not necessarily need to be in KEP form, and/or it can be of different type for $C_{\rho e}$ and $C_{\rho k}$. Also, a different variable can be evolved in place of total energy. The numerical treatment of the energy equation and the associated conservation properties are extensively discussed in a recent paper in the context of ideal-gas thermodynamics [49].

In this regard, besides recent interest on the PEP property (discussed in the next section) many research efforts have been devoted over the lasts decades to enforce discrete conservation of entropy. This is indeed a strong physics-based proxy of non-linear stability for compressible flows, especially in the presence of shocks, to ensure correct production of entropy and convergence towards weak solutions. In the context of linear split-based formulations such as those considered in this work, Honein and Moin [50] proposed to evolve entropy instead of total energy, thus obtaining a scheme that is KEP and entropy-preserving, but did not conserve total energy. More recently, the kinetic-energy and entropy-preserving (KEEP) scheme proposed in [24] corresponds to discretizing the internal energy equation with its convective term expressed in KGP form. This scheme satisfies additional analytical relations in terms of internal/kinetic energy exchange at the discrete level, and has favorable entropy-conservation properties, although it is strictly not fully entropy preserving [25]. Both approaches have shown that enforcing discrete entropy conservation (even approximately) in addition to KEP can lead to enhanced fidelity and robustness of turbulent compressible flow simulations, also in the absence of shocks. Using Tadmor-type [40] flux functions, a KEP numerical flux that conserves total energy, entropy and is PEP was recently proposed for ideal gases [30]. Since the present study focuses on low-Mach number turbulent flows with a (pseudo-)interface, the main focus was devoted on enforcing the KEP and PEP properties; entropy conservation has not been taken into consideration and might be part of future work.

3.1.2. PEP conditions

The second component of the novel framework is the enforcement of the PEP condition introduced in Section 1. This property can be easily demonstrated in a continuous setting by considering the one-dimensional velocity-evolution equation, which can be derived by subtracting the mass equation multiplied by velocity from the momentum equation, yielding

$$u_t = -\frac{1}{\rho}\left[\frac{\partial}{\partial x}(\rho u u) + \frac{\partial P}{\partial x} - u\frac{\partial}{\partial x}(\rho u)\right], \tag{14}$$

and a one-dimensional, inviscid version of the general pressure evolution equation, Eq. (4),

$$P_t = -\frac{\partial}{\partial x}(Pu) - (\rho c^2 - P)\frac{\partial u}{\partial x}. \tag{15}$$

Based on Eqs. (14)-(15), it can be immediately deduced that when the initial pressure and velocity are spatially constant (with density varying in space), i.e., $u = \bar{u}$ and $P = \bar{P}$, then neither pressure nor velocity change in time; it is therefore highly desirable that this equilibrium is discretely preserved also in numerical simulations. From a physical standpoint, this equilibrium condition arises and is of crucial importance in any situation that involves a material interface with no pressure jumps, for instance multi-phase interfaces with no or negligible surface tension (i.e., in the limit of high Weber numbers), multi-component mixing (a fundamental process in reactive systems) or, as in the present study, pseudo-interfaces that generate when a fluid crosses the pseudo-boiling line. Numerical methods generally fail to reproduce the PEP property discretely, even when the variation of the thermo-fluid-dynamic properties across the interface is smooth (as assumed in this study), and regardless of the thermodynamic model.

While the KEP property depends exclusively on how the continuity and momentum equations are discretized, the fulfilment of the PEP property depends directly on the choice of the energy variable, and how the corresponding equation is numerically treated. When the total or the internal energy are directly discretized, the pressure equation is an *induced* equation, and whether $u_t = 0$ and $P_t = 0$ are satisfied or not has to be verified on a case-by-case basis by deriving the corresponding discrete evolution equations for velocity and pressure. In a pressure-equilibrium framework, i.e., when $u = \bar{u}$, it is useful to preliminarily

observe that *any* combination of the split forms in Eq. (9) reduces to

$$C_\rho = \bar{u}\delta_x\rho; \quad C_{\rho u} = \bar{u}^2\delta_x\rho; \quad C_{\rho k} = \frac{\bar{u}^3}{2}\delta_x\rho. \tag{16}$$

The induced discrete equation for velocity reads:

$$u_t = -\frac{1}{\rho}\left(C_{\rho u} - \bar{u}C_\rho + \delta_x\bar{P}\right) \tag{17}$$

which, in light of Eq. (16), is easily seen to satisfy $u_t = 0$ for any choice of the split forms for C_ρ and $C_{\rho u}$.

The induced pressure equation can instead be obtained by time-differentiating the equation of state and applying the chain rule with respect to the time variable,

$$P_t = P_\rho\rho_t + P_e e_t = P_\rho\rho_t + \frac{P_e}{\rho}[(\rho e)_t - e\rho_t]. \tag{18}$$

The behaviour of the induced Eq. (18) depends on the discretization of the energy equation (i.e., choice of the energy variable and corresponding numerical treatment). In the following, two cases will be firstly considered in which the total energy and the internal energy equations are directly discretized. Finally, the case in which an evolution equation for pressure is utilized will be discussed.

Total energy equation. The first class of methods under consideration is one where the total energy equation, Eq. (8c), is directly discretized. In this case, the internal energy evolution is in turn an induced equation, which can be obtained by subtracting the (induced) discrete kinetic energy equation to Eq. (8c), yielding

$$\begin{aligned}(\rho e)_t = (\rho E)_t - (\rho k)_t = (\rho E)_t - \left[u(\rho u)_t - \frac{u^2}{2}\rho_t\right] = \\ = -\left[C_{\rho e} + C_{\rho k} - \left(uC_{\rho u} - \frac{u^2}{2}C_\rho\right)\right] - \left[\Pi_{\rho E} - u\delta_x P\right].\end{aligned} \tag{19}$$

Upon substituting Eq. (16) into Eq. (19), and then into Eq. (18), and taking into account that pressure and velocity are constant in the PEP framework, the induced pressure equation reads

$$P_t = \left[\frac{P_e}{\rho}e - P_\rho\right]\bar{u}\delta_x\rho - \frac{P_e}{\rho}\left[C_{\rho e} + \Pi_{\rho E}\right]. \tag{20}$$

In order to further develop Eq. (20) and verify the fulfilment of the PEP condition, a choice has to be made regarding the discretization of the terms $\Pi_{\rho E}$ and $C_{\rho e}$. For the former, it is straightforward to notice that Eq. (12) is in PEP form for any value of η, while Eq. (13) is PEP only if discretized using the divergence form. Upon inspection, the method KGP-Et is thus easily seen to be not PEP. Regarding the latter term, under the assumption of constant velocity, its expansion again reduces to the combination of *conservative* and *advective* formulations:

$$C_{\rho e} = \chi\bar{u}\delta_x(\rho e) + (1-\chi)\bar{u}(e\delta_x\rho + \rho\delta_x e). \tag{21}$$

However, any value of $\chi \neq 0$ leads to the presence of the term $\delta_x(\rho e)$, which cannot be further manipulated for general equations of state and for lack of a discrete product rule. On the contrary, by picking $\chi = 0$ and plugging Eq. (21) into Eq. (20), and by further assuming that $\Pi_{\rho E} = 0$, one is left with

$$P_t = -\bar{u}(P_\rho\delta_x\rho + P_e\delta_x e) \approx -\bar{u}\delta_x\bar{P} = 0. \tag{22}$$

The approximate equality in the r.h.s. of Eq. (22) is related to the discrete fulfilment of the chain rule with respect to space. Second-order centered derivative operators satisfy a discrete version of the chain rule [51]:

$$\delta_x P = \widetilde{P_\rho}\delta_x\rho + \widetilde{P_e}\delta_x e, \tag{23}$$

where $\widetilde{P_\rho}$ and $\widetilde{P_e}$ are possibly non-linear operators acting on the Jacobian functions. Compared to their continuous counterparts, the discrete Jacobians are second-order accurate for interior nodes. Importantly, the result in Eq. (23) cannot be generalized to higher-order derivative operators [51]. In summary, algorithms based on the direct discretization of the total energy equation that employ:

- Eq. (21) for $C_{\rho e}$ with $\chi = 0$, which in turn implies any linear combination of $C^{\phi}_{\rho e}$ and $C^{\rho}_{\rho e}$;
- *any* split form for $C_{\rho k}$;
- Eq. (12) for $\Pi_{\rho E}$ with any value of η or Eq. (13) in divergence form,

require the sole discrete reproduction of the chain rule by the spatial differential operator to accomplish the PEP property. All the other combinations, including the method KGP-Et, require the product rule to be also discretely invoked. This class of schemes is hereinafter labeled as CR (chain rule). In this work, one specific scheme is selected for numerical testing, in which the KGP formulation is used for C_{ρ}, $C_{\rho u}$, $C_{\rho k}$, while $C_{\rho e} = C^{\phi}_{\rho e}$, and $\eta = 1$; this scheme is labeled as KGP-Et-CR.

It is worth to observe that in the case of the ideal-gas equation of state, i.e., $P = (\gamma - 1)\rho e$, then $P_{\rho} = (\gamma - 1)e$ and $P_e = (\gamma - 1)\rho$, leading to cancellation of the first term in the r.h.s. of Eq. (20). Therefore, the PEP requirement in this case simplifies to $C_{\rho e} + \Pi_{\rho E} = 0$, as previously reported [52]; this condition can be satisfied in several ways. Upon leveraging the linear relation between P and ρe for ideal gases, the contribution due to $C_{\rho e}$ can be cancelled by splitting this term based on a linear combination of $C^{D}_{\rho e}$ and $C^{u}_{\rho e}$. Accordingly, Shima et al. [10] recently proposed a PEP scheme for ideal gases where $C_{\rho e} = (C^{D}_{\rho e} + C^{u}_{\rho e})/2$, with every other term discretized as in the previously proposed KEEP scheme; this scheme is labeled as PEP-IG.

Finally, it is worth noticing that if ρe is chosen as a state variable instead of e, i.e., $P = P(\rho, \rho e)$, similar conclusions can be achieved for the case of general equations of state. However, in this case, $\chi = 1$ should be used in Eq. (21) to get to Eq. (22), and the resulting split form would be PEP for ideal gases.

Internal energy equation. If the internal energy equation,

$$(\rho e)_t = -C_{\rho e} - P\delta_x u, \tag{24}$$

is directly discretized in place of Eq. (8c), the induced pressure equation becomes

$$P_t = \left[\frac{P_e}{\rho} e - P_{\rho}\right] \bar{u}\delta_x \rho - \frac{P_e}{\rho} C_{\rho e}. \tag{25}$$

Similar conclusions can be obtained as those already drawn for the previous approach in which total energy is directly discretized. In particular, when $C_{\rho e}$ is split using $\chi = 0$, the resulting method only requires the discrete application of the chain rule to enforce the PEP condition; otherwise, the product rule also needs to be used. The scheme selected for testing is based on $C_{\rho e} = C^{\phi}_{\rho e}$, and is labeled KGP-et-CR. Of note, schemes based on the internal energy equation are total-energy conserving (TEC), as long as a KEP method is used, if $C_{\rho e}$ is discretized using a locally-conservative formulation, and the induced pressure term results in an advective formulation of $\delta_x pu$. This latter condition is true as long as the pressure term in the internal energy equation is discretized as in Eq. (24), and the derivative matrices acting on u and p satisfy a reciprocal skew-symmetric relationship [52]. The same derivative operator is used for all terms in this work, thus the condition is indeed satisfied. Hence, KGP-et-CR is also TEC.

Pressure equation. Finally, the case in which the pressure equation is evolved in place of Eq. (8c) is analyzed. A one-dimensional, inviscid, semi-discrete version of Eq. (4) reads

$$P_t = -C_p - (\rho c^2 - P)\delta_x u, \tag{26}$$

where $C_p = \delta_x(Pu)$; therefore, the family of split forms in Eq. (12) also applies to C_p. Obviously, for constant pressure and velocity, any value of η will lead to $P_t = 0$. The case $\eta = 0$ is selected and the corresponding PEP scheme is labeled as KGP-Pt.

In this case, however, total energy conservation is sacrificed; indeed, both the discrete chain and the product rules are needed to demonstrate TEC, regardless of the split forms considered. This can be shown

by deriving the induced total energy equation, as the sum of the induced discrete evolution equations of internal and kinetic energy. Isolating $(\rho e)_t$ from Eq. (18), and adding the contribution of $(\rho k)_t$, one gets to

$$(\rho E)_t = \overbrace{\frac{\rho}{P_e}(P_t - P_\rho \rho_t) + e\rho_t}^{(\rho e)_t} + \underbrace{\left(uC_{\rho u} - \frac{u^2}{2}C_\rho\right) - u\delta_x P}_{(\rho k)_t}. \tag{27}$$

Substituting Eq. (26) with $\eta = 0$, using Eq. (23), and taking into account that $c^2 = P_\rho + P/\rho^2 P_e$, yields:

$$(\rho E)_t = -\overbrace{\left(\frac{\widetilde{P_e}}{P_e}\rho u\delta_x e + eC_\rho\right)}^{P_1} - \overbrace{\left(uC_{\rho u} - \frac{u^2}{2}C_\rho\right)}^{P_2} - \underbrace{(u\delta_x P + P\delta_x u)}_{P_3} + \overbrace{\rho\frac{P_\rho}{P_e}\left(C_\rho - \frac{\widetilde{P_\rho}}{P_\rho}u\delta_x\rho - \rho\delta_x u\right)}^{P_4}. \tag{28}$$

Demonstrating conservation of total energy is equivalent to show that the r.h.s. of Eq. (28) can be expressed in a locally conservative formulation (i.e., as a difference of fluxes). The terms P_1, P_2 and P_3 are the induced contributions of internal energy, kinetic energy and pressure, while P_4 is a spurious error term. In particular, P_2 is in locally conservative form for any KEP scheme belonging to the class discussed in this paper; P_3 is an advective instance of the product $\delta_x(Pu)$, and thus can also be recast as a difference of fluxes [23]. However, the chain rule in space needs to be satisfied exactly (i.e., $\widetilde{P_e} = P_e$ and $\widetilde{P_\rho} = P_\rho$) to potentially satisfy TEC. Even in this case, the product rule is also necessary: if $C_\rho = C_\rho^u$, then $P_4 = 0$, but P_1 provides $C_{\rho e}^L$, which is a non-conservative split form. On the other hand, selecting $C_\rho = C_\rho^D$, the induced internal energy contribution becomes of type $C_{\rho e}^\phi$, hence conservative, but the product rule is again needed to eliminate P_4. It is important to remark that the induced kinetic energy balance is independent of the discretization of the energy equation, and is preserved for KEP schemes. Therefore, the lack of conservation of total energy is only associated with an incorrect (induced) discrete internal energy balance.

3.1.3. Summary of KEP and PEP schemes

Table 1 summarizes a subset of notable schemes emerged from the previous theoretical analysis, which have been selected for further numerical assessment. All the schemes are based on the KGP split form for the convective terms in the continuity and the momentum equations, and as such they all preserve mass, momentum and kinetic energy both globally and locally.

In the scheme labeled KGP-Et, the total energy is directly solved for, and the KGP split is applied to enthalpy (i.e., the convective and pressure terms in the total energy equation are combined); this scheme has been previously proposed and used in, e.g., [22, 53]. Upon deriving the induced equation for pressure, it is shown that this method requires application of both the product and the chain rules to be PEP. On the other hand, a careful choice of the split formulation for $C_{\rho e}$ in the total energy equation leads to a class of schemes that would be PEP if the chain rule alone was discretely satisfied by the spatial derivative operator. One particular instance of this class of schemes, named KGP-Et-CR, has been selected for testing. Of note, the specific split family to be chosen for $C_{\rho e}$ to obtain this class of schemes depends on the choice of the thermodynamic state-variables pair. Similar results are obtained if the internal energy is directly discretized; a method from this family, called KGP-et-CR, is proposed for testing. Notice that there is a subtle difference between the schemes KGP-Et-CR and KGP-et-CR, stemming from the induced kinetic-energy and pressure terms. In other words, if $C_{\rho k}$ and $\Pi_{\rho E}$ in the KGP-Et-CR were discretized *à la* KEEP, as proposed by Kuya et al. [24], the two methods would be identical. This difference is deliberately kept in this work to observe the different numerical behaviour, and for consistency with the *reference* KGP-Et scheme.

In summary, the discrete chain rule appears to constitute a *barrier* for the development of PEP methods, at least for discretizations based on linear finite-differencing schemes. Based on current knowledge, a discrete form of the chain rule is only available for second-order differential operators, and is satisfied to $\mathcal{O}(h^2)$. To overcome this barrier, a class of schemes is proposed and analyzed in which pressure is evolved in place of total or internal energy. In this case, the PEP condition can be easily satisfied, but a formal analysis

Label	Energy	$C_{\rho e}$	$C_{\rho k}$	$\Pi_{\rho E}$	C_p	TEC	PEP
KGP-Et	Eq. (8c)	$C_{\rho e}^{\mathrm{KGP}}$	$C_{\rho k}^{\mathrm{KGP}}$	$C_{\rho \hat{p}}^{\mathrm{KGP}}$	–	✓	×
KGP-Et-CR	Eq. (8c)	$C_{\rho e}^{\phi}$	$C_{\rho k}^{\mathrm{KGP}}$	$\eta = 1$	–	✓	◯
KGP-et-CR	Eq. (24)	$C_{\rho e}^{\phi}$	–	–	–	✓	◯
KGP-Pt	Eq. (26)	–	–	–	$\eta = 0$	×	✓
PEP-IG	Eq. (24)	$(C_{\rho e}^{D} + C_{\rho e}^{u})/2$	$C_{\rho k}^{\mathrm{KGP}}$	–	$\eta = 0$	✓	×

Table 1: Discretization and properties of the selected formulations considered in this work. In all cases, the continuity and momentum equations are assumed to be discretized with a KGP form. ✓: condition satisfied; ×: discrete product and chain rules are needed; ◯: only chain rule is needed. This table refers to a general equation of state $P = P(\rho, e)$.

shows that discrete total energy conservation is sacrificed. The resulting approach, which combines the KGP scheme with the solution of an evolution equation for pressure, is, to the best of the authors' knowledge, novel, and has been labeled KGP-Pt. In Section 4, the schemes listed in Table 1 will be numerically assessed and compared with *standard* methods, briefly summarized in the next section.

3.2. Existing methods for supercritical fluids turbulence

This sections briefly describes several existing approaches commonly employed for solving the equations of fluid motion for compressible flow, and in some cases schemes that have been specifically tailored for trans-/supercritical regimes. Three representative categories are taken into consideration, as reported in the following, which will be numerically tested in this study for comparison with the novel schemes.

3.2.1. Conservative method with stabilization

This class is representative of a rather "traditional" approach in the compressible flow community, which consists in solving the classical set of governing equations, Eqs. (1), with all the convective terms discretized in divergence formulation. This approach is hereinafter labeled as D. It is inherently unstable in multi-scale simulations due to lack of KEP (see also Section 3.1.1), and thus it is typically coupled with a stabilization method, e.g., low-pass filtering. In this work, the focus is placed on a class of implicit filters initially proposed by Lele [54] and later exploited by Visbal and Gaitonde [17], where each conservative variable is filtered according to

$$\alpha_f \bar{\varphi}_{i-1} + \bar{\varphi} + \alpha_f \bar{\varphi}_{i+1} = \sum_{n=0}^{N_f} \frac{a_n}{2} (\varphi_{i+n} + \varphi_{i-n}), \tag{29}$$

where $\bar{\varphi}$ is the filtered variable and a_n the filter coefficient parameters. A fourth-order filter, F4, with $\alpha_f = 0.495$ and the corresponding filter coefficients $a_0 = 5/8 + 3/4\alpha_f$, $a_1 = 1/2 + \alpha_f$ and $a_2 = -1/8 + 1/4\alpha_f$ is employed at each Runge-Kutta stage and at each time step, without changing the filter coefficients; the resulting method is labeled D+F4. Low-pass filters introduce numerical dissipation, but are generally successful in stabilizing the solution when a non-linearly unstable scheme is used. On the other hand, as reported in [16], filtering can amplify pressure oscillations due to the interaction with thermodynamic non-linearities, particularly across the pseudo-boiling line. Even though increasing the order of the filter obviously leads to a less dissipative filter, here the stencil is limited to a four-point function for efficiency purposes; indeed, increasing the stencil width is known to significantly deteriorate parallel computational performances, especially when dealing with implicit spatial schemes [55]. Methods of this class (although of higher spatial order) have been previously used for supercritical simulations in, e.g., [56]. Finally, it is worth to note that when the filter coefficients are not re-scaled according to the time step size, this is known to introduce a temporal inconsistency in terms of how much dissipation is added to the solution, with potential risks of over-dissipation. In this regard, temporally-consistent filtering techniques, such as those proposed in [57, 58], might be considered for future work.

Label	Ref.	Energy	$C_{\rho\phi}$	$\Pi_{\rho E}$	C_p	Notes
D	–	Eq. (8c)	$C^{\mathrm{D}}_{\rho\phi}$	$\eta = 1$	–	Unstable; only used for comparison
D+F4	[56]	Eq. (8c)	$C^{\mathrm{D}}_{\rho\phi}$		–	Use of Eq. (29) with $\alpha_f = 0.495$ and $N_f = 1$
D-Pt+F4	[14]	Eq. (26)	$C^{\mathrm{D}}_{\rho\phi}$	–	$\eta = 1$	Use of Eq. (29) with $\alpha_f = 0.495$ and $N_f = 1$
UB-Df	[13]	Eq. (8c)	HLLC[4]	$\eta = 1$	–	Use of double-flux method
KGP-Df	novel	Eq. (8c)	$C^{\mathrm{KGP}}_{\rho\phi}$		–	Use of double-flux method

Table 2: Summary of existing schemes for transcritical flows assessed in this work. The last row is a novel combination. In the column for $C_{\rho\phi}$, it is assumed that the same scheme is used for *any* variable ϕ.

3.2.2. Pressure-based approach in divergence formulation

As mentioned in Section 1, solving an equation for pressure to have better control of spurious pressure oscillations has been previously proposed by, e.g., Terashima and Koshi [14]. However, convection was otherwise discretized using the divergence formulation. As a representative scheme of this class, a method analogous to D+F4 is tested, but in which pressure is solved instead of total energy, called D-Pt+F4.

3.2.3. Double-flux methods

The double-flux approach [12] was recently extended to supercritical flows by Ma et al. [13]. In this method total energy is discretized, but the internal energy is fixed within the time-integration step to artificially enforce pressure equilibrium. If the relationship between internal energy and pressure for real gases is generically rewritten as $\rho e = P/(\gamma^* - 1) + e_0^*$, where e_0^* and γ^* are non-linear functions of the thermodynamic states, then in the double-flux approach γ^* and e_0^* are "frozen" both in space and time during each time step; details can be found in [13], where the solution was found to be free of spurious pressure oscillations. The double-flux approach has been typically coupled with upwind-biased schemes; here, following [13], it will be tested in conjunction with the HLLC scheme [59]; the resulting method has been labeled UB-Df (upwind-biased double-flux). The PEP property in this case is obviously achieved at the expenses of KEP. For the sake of comparison, the double-flux method will be also assessed for the first time in conjunction with the KGP-Et scheme, here denoted as KGP-Df.

4. Numerical results

The rationale for the design of the numerical tests was to first (i) verify the theoretical framework and assess the PEP and TEC properties for all the proposed schemes, along with the asymptotic behaviour of the corresponding errors, using a 1D inviscid advection of a density wave, as previously proposed in Bernades et al. [60]; then (ii) to investigate the importance of enforcing the PEP property in a multi-dimensional context, by inspecting the local quality of the flow field for a 2D multiphase problem, i.e., an inviscid mixing layer under transcritical conditions, simulated by a state-of-the-art KEP scheme (KGP-Et) in comparison with the novel pressure-based KEP+PEP scheme (KGP-Pt); finally (iii) apply the KGP-Pt scheme to a complex turbulent flow, particularly the direct numerical simulation (DNS) of a transcritical channel flow.

4.1. 1D advection of a density wave

The main objectives of this test are to: (i) verify the TEC and PEP theoretical predictions presented in Table 1 for the KEP schemes; (ii) assess the overall behaviour of all the schemes presented in Table 1

[4]In this case, the HLLC scheme is used for the discretization of the convective terms C_ρ, $C_{\rho u}$ and $C_{\rho E}$.

and Table 2; and (iii) verify the asymptotic behaviour of the TEC and PEP errors. To this end, following previous works [10, 13], the inviscid one-dimensional advection of a density wave,

$$\rho(x, t = 0) = \frac{\rho_{min} + \rho_{max}}{2} + \left(\frac{\rho_{max} - \rho_{min}}{2} \right) \sin(2\pi x), \tag{30}$$

is simulated at constant velocity $v_0 = 1\,\mathrm{m/s}$. Despite its simplicity, this test has proven to be very challenging for standard numerical schemes, as it is highly sensitive to the generation of spurious pressure oscillations. With the aim of testing the theoretical framework in a consolidated context, ideal-gas conditions will be analyzed first. Then, results for transcritical conditions with real-gas thermodynamics will be presented.

4.1.1. Ideal-gas thermodynamics

In low-pressure, ideal-gas conditions, the 1D advection test is performed with the following setup: reference bulk pressure of $P_0 = 1\,\mathrm{Pa}$, $\rho_{min} = 1\,\mathrm{kg/m^3}$ and $\rho_{max} = 3\,\mathrm{kg/m^3}$, with reference $\rho_0 = 2\,\mathrm{kg/m^3}$. The domain length is $L = 1\,\mathrm{m}$, discretized with 41 equally-spaced grid points and acoustic CFL= 0.3. The flow is advanced up to $t/t_c = 11$ ($t_c = 1s$) using a standard fourth-order Runga-Kutta time integrator. From Table 1, only KGP-Et and KGP-Pt were tested, as the other schemes were specifically developed for general equations of state; in addition, Shima et al.'s method [10] (PEP-IG) was also included for comparison. From Table 2, double-flux does not apply in this case, hence UB-Df and KGP-Df become simply UB and KGP-Et; also, filtering was not used in this case, because (i) this test is not susceptible to aliasing-related instabilities, and (ii) the D-based schemes are PEP for ideal gases (see Section 3.1.2). Finally, another method (hybrid, H), where the sensor proposed by Ducros et al. [61] is used to switch between KGP and HLLC, was also tested.

Two main conclusions can be drawn from the results shown in Figure 1. First, only three schemes are free from pressure oscillations: D, in accordance with the theoretical framework (however, this scheme is not KEP and is generally unstable for multi-dimensional flows), PEP-IG and the novel KGP-Pt. The KGP-Et is not PEP and indeed suffers from spurious pressure oscillations, which in turn affect the thermophysical quantities. On the other hand, dissipative methods minimize these oscillations, although not completely, as seen for H in the detailed zoom area from Figure 1(b). The second (expected) conclusion is that the UB scheme leads to dissipation of the density wave, while the hybrid H scheme is dissipating at a slightly lower rate. It should be noted, however, that the sensor is mostly active as a result of the oscillations, and the upwind-biased scheme is governing the discretization of the convective term. In all cases, the density field suffers from a time lag due to the dispersion error of the second-order scheme.

4.1.2. Real-gas thermodynamics

A transcritical 1D advection test is simulated, as previously proposed by Ma et al. [13]. The test is carried out with the same domain length, mesh size and time integrator as in the ideal-gas case. In this case, N_2 is the supercritical fluid operating at bulk (constant) pressure of $P_0 = 5\,\mathrm{MPa}$ and advected at initial constant velocity $u_0 = 1\,\mathrm{m/s}$. The density profile is assigned with $\rho_{min}/\rho_c = 0.182$ ($T = 300\,\mathrm{K}$) and $\rho_{max}/\rho_c = 2.531$ ($T = 100\,\mathrm{K}$), with reference density $\rho_0/\rho_c = 0.305$ ($T = 200\,\mathrm{K}$).

Numerical results are depicted in Figure 2. All the schemes listed in Table 1 and Table 2 are tested, with the exception of D and with the addition of PEP-IG. Six main conclusions can be drawn: (i) as theoretically anticipated, KGP-Et is not PEP, while the schemes of the CR family do not seem to offer practical advantages in terms of mitigating pressure oscillations; (ii) the PEP-IG scheme is not PEP for real-gas equations of state, as better highlighted in the zoomed inset plot in Figure 2(b), (iii) the double-flux formulation is apparently able to prevent the amplification of pressure disturbances only if it is coupled with an upwind-biased (UB) method, whereas the pressure equilibrium is altered when the Df is used in conjunction with the KGP method; (iv) filtering is unable to suppress pressure oscillations; also, disturbances are particularly severe when crossing the pseudo-boiling line at $x/L \approx 0.65 - 0.85$, in accordance with previous results showing that filters may amplify pressure oscillations due to the interaction with non-linear thermodynamics [16]; (v) dissipative methods alter the thermodynamic properties [i.e., density in Figure 2(a)], especially UB-Df. A small amount of dissipation is present even when utilizing a low-dissipative filter, D+F4; and (vi) pressure equilibrium is maintained only for D-Pt+F4 and for the novel KGP-Pt.

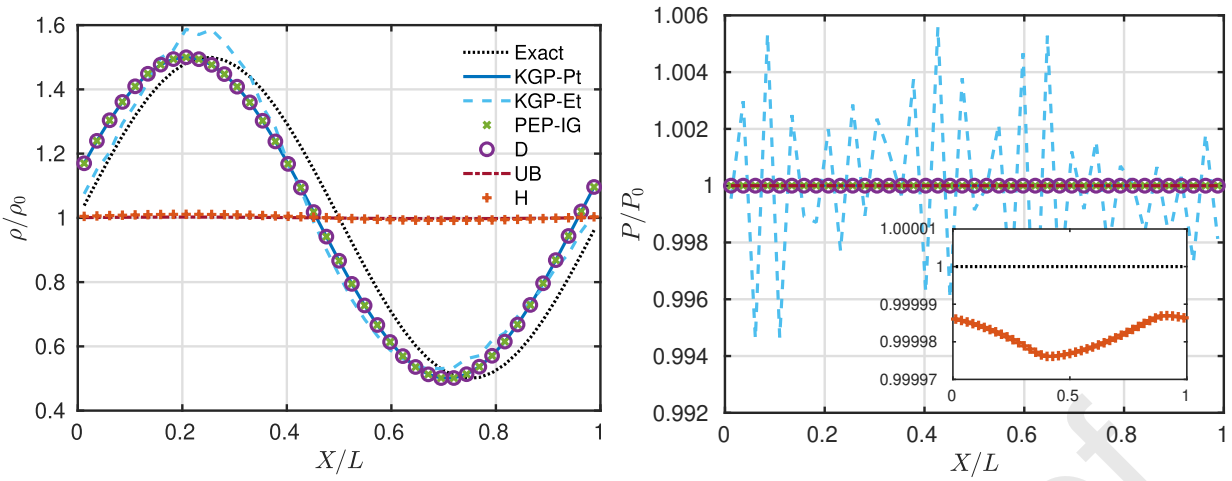

(a) (b)

Figure 1: 1D advection test under ideal-gas conditions ($\gamma = 1.4$), at $t/t_c = 11$, for several schemes (see text and tables for details). Shown are normalized (a) density and (b) pressure.

In addition, a grid-refinement study was performed to analyze the asymptotic behaviour of the error for the conservation of total energy (in the case of the KGP-Pt scheme) and of pressure-equilibrium preservation. In particular, the following quantities are introduced:

$$\varepsilon_{\mathrm{TEC}} = |\langle\overline{\rho E}\rangle|, \qquad \varepsilon_{\mathrm{PEP}} = \|P(x, t = t_f) - P_0\|_2, \tag{31}$$

where t_f is the final time of integration, $\|\cdot\|_2$ is the L_2 norm, the overline $\overline{f}$ indicates integration over the spatial domain and the operator $\langle f\rangle$ is defined, for a generic variable f, as

$$\langle f\rangle = \frac{f(x, t = t_f) - f(x, t = 0)}{f(x, t = 0)}. \tag{32}$$

Figure 3 shows the error quantities defined in Eq. (31) for the schemes from Table 1. Total energy is preserved to machine accuracy for schemes based on total or internal energy, in accordance with the theoretical analysis, while it appears to follow (on average) a scaling of type $\mathcal{O}(h^2)$ for KGP-Pt, as reported in Fig. 3(a). Importantly, the total energy decreased in all cases [Fig. 3(a) reports the absolute value]. On the other hand, Fig. 3(b) shows that the PEP error $\varepsilon_{\mathrm{PEP}}$ is also (mostly) second-order accurate, except in the first and last tracts of the KGP-Et-CR and KGP-Et, respectively. This behaviour is assumed to be associated with the unstable character of the pressure oscillations, that hamper the achievement of a *pure* asymptotic behaviour. The schemes KGP-Et and KGP-et-CR behave similarly (at least up to $h = 0.025\,\mathrm{m}$), while the KGP-Et-CR method provides PEP errors of several orders of magnitude higher than the other schemes. As elaborated in Section 3.1.3, the KGP-et-CR can be interpreted as a version of KGP-Et-CR in which the consistency of the internal and kinetic energy fluxes is also enforced, similarly as done in [24]. This could explain the better behaviour of the internal-energy based method compared to the total energy one. Based on the results of this 1D test, two schemes are isolated for further assessment: the novel KGP-Pt (the only one to be simultaneously KEP and PEP) and a reference KEP scheme, KGP-Et.

4.2. 2D inviscid transcritical mixing layer

The overall numerical stability and practical benefits of the newly proposed scheme KGP-Pt are here demonstrated for a two-dimensional inviscid transcritical mixing layer, as compared with a reference KEP and TEC method such as KGP-Et. A 2D mixing layer of N_2 is simulated in a domain $x \in [-0.5, 0.5]$ and $y \in [-0.25, 0.25]$ discretized with 256×128 uniformly spaced grid points, corresponding to $h = 0.0039\,\mathrm{m}$. The mixing layer is defined by setting a temperature difference between top $T/T_c = 0.75$ and bottom $T/T_c = 1.5$

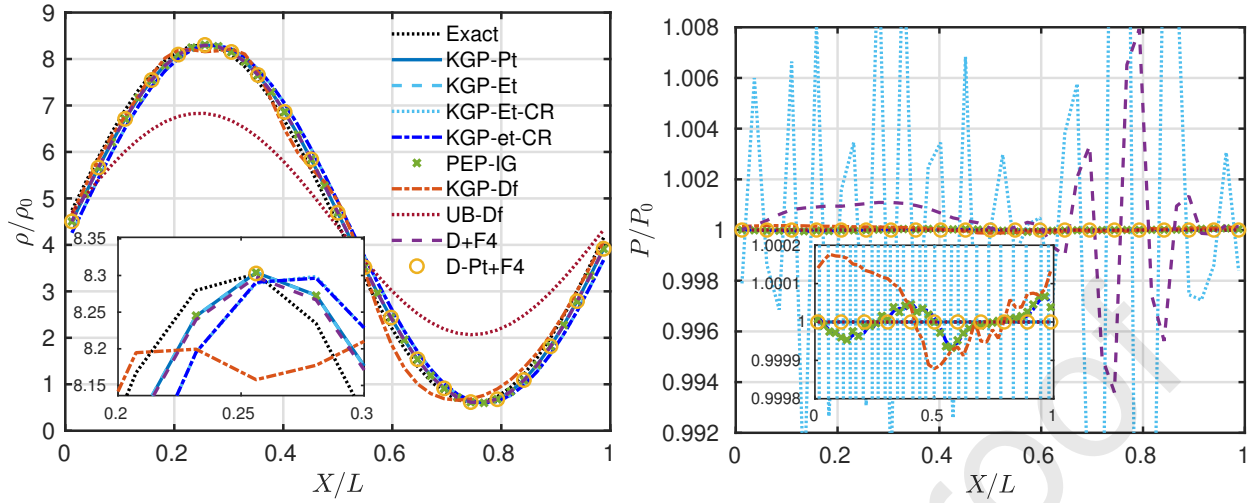

(a) (b)

Figure 2: 1D advection test under transcritical thermodynamic conditions, at $t/t_c = 10^{-2}$, for several schemes (see text and tables for details). Shown are normalized (a) density and (b) pressure.

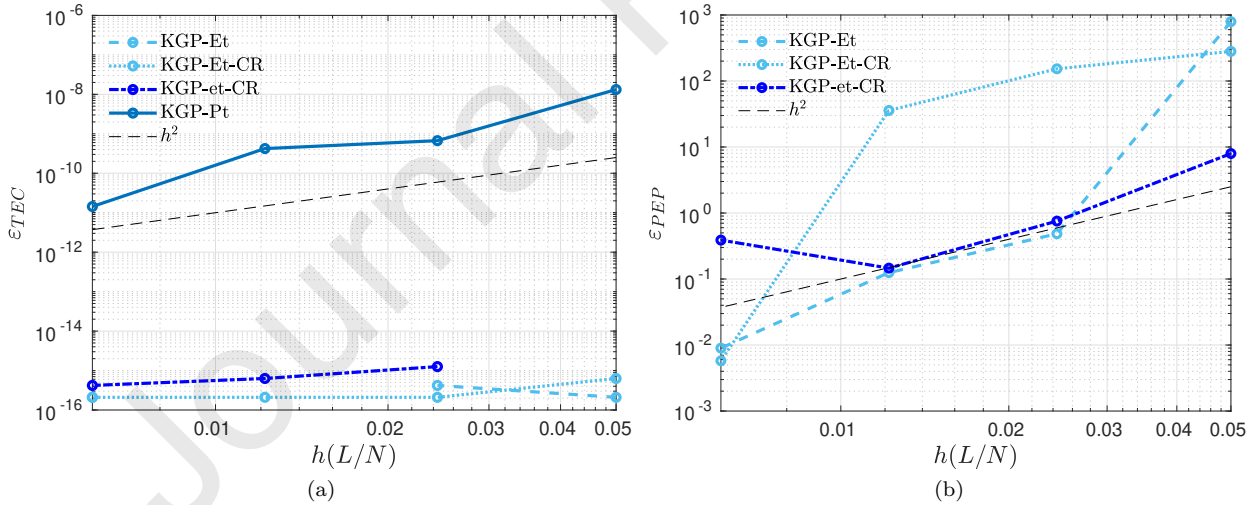

(a) (b)

Figure 3: Results of grid-refinement study for the 1D advection test under transcritical thermodynamic conditions. Errors (a) $\varepsilon_{\mathrm{TEC}}$ and (b) $\varepsilon_{\mathrm{PEP}}$ at $t/t_c = 10^{-2}$ for several schemes (see text and tables for details).

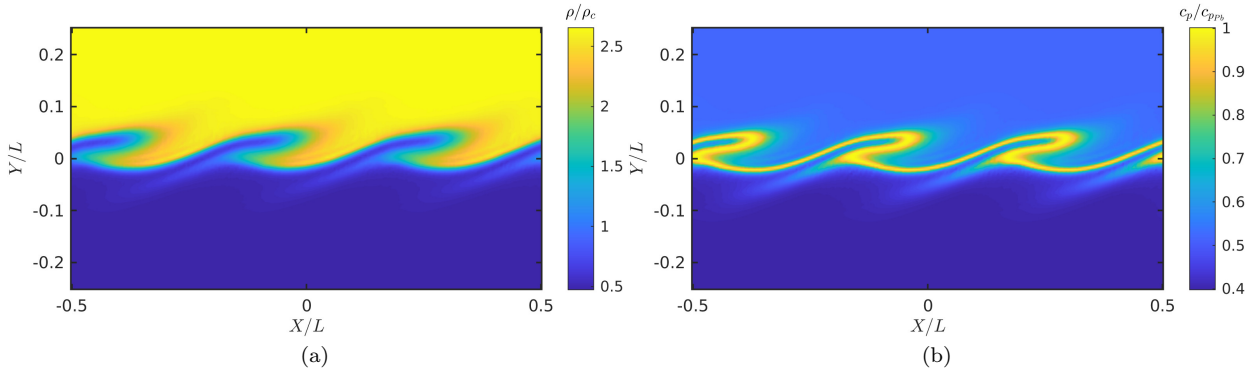

(a) (b)

Figure 4: 2D inviscid transcritical mixing layer at $t/t_c = 2$. Results were obtained using the KGP-Pt scheme, 256×128 mesh size with CFL= 0.3. Contours of normalized (a) density and (b) c_p with respect to critical point values.

boundaries, and a bulk pressure of $P/P_c = 2$. The left and right boundaries are periodic, whereas for the top and bottom ones a symmetry condition is imposed for the vertical velocity and a homogeneous Neumann condition is prescribed for all the other conserved variables. The initial condition is defined as

$$\begin{cases} u = u_0[1 + A_u \tanh(\bar{\delta} y)], \\ v = 0, \\ T = T_c[3A_t - A_t \tanh(\bar{\delta} y)], \end{cases} \tag{33}$$

with $A_t = A_u = 3/8$ and $u_0 = 25\,\mathrm{m/s}$. These values, along with the factor $\bar{\delta} = 20$, establish that the velocity and temperature fields change from bottom- to top-boundary values within $y = \pm 0.1\,\mathrm{m}$. In order to trigger the Kelvin-Helmholtz (KH) instability, perturbations are applied on the velocity field within the region in which the profiles change from bottom- to top-boundary values [62]. The perturbation field $\mathbf{u}_p = [U_p, V_p]$ is defined as a superposition of sinusoidal- and random-based functions as

$$U_p = V_p = a_y[\sin(k\pi x) + a_g g(x)], \tag{34}$$

where $a_y = \Delta u[e^{-(y-L_y/2)^2/\theta} + e^{-y^2/\theta} + e^{-(y+L_y/2)^2/\theta}]$, $k = 6$ in order to trigger 3 vortices roll-ups within the domain (wavelength $\lambda = 1/k = 1/3\,\mathrm{m}$), the amplitude of the fluctuations is set to $a_g = 1/10$, and $g(x)$ is the randomly-defined perturbation with values varying in the range $[-0.5, 0.5]$ across the x-direction. Finally, $A = 0.1$ is the amplitude factor reduction, $\Delta u = 10\,\mathrm{m/s}$ is the difference between bottom and top boundaries, and θ is the momentum thickness defined as

$$\theta = \int_{-L_y/2}^{L_y/2} \frac{u(y) - u_{bw}}{\Delta u} \left(1 - \frac{u(y) - u_{bw}}{\Delta u}\right) \mathrm{d}y, \tag{35}$$

where the bottom boundary velocity is $u_{bw} = 20\,\mathrm{m/s}$.

Figure 4(a) shows a contour of the density field at $t/t_c = 2$, where $t_c = \lambda/\Delta u = 2/(k\Delta u) = 0.033$ s, obtained with the KGP-Pt scheme. The typical KH rollers have developed and are starting to promote the mixing of the liquid-like layer (top) and the gas-like layer (bottom). Fig. 4(b) highlights the narrow range close to the pseudo-boiling line (max c_p) where highly non-linear thermodynamic changes occur.

A detailed analysis of the time evolution of several integral quantities up to $t/t_c = 2$, provided by the novel KGP-Pt scheme, is shown in Fig. 5; all the quantities are reported according to the normalization given in Eq. (32). Mass and momentum are preserved to machine accuracy [see Figs. 5(a)-(b)], while Fig. 5(c) shows that total energy is not conserved, as anticipated by the theoretical analysis and as also reported in the previous subsection. Since KGP-Pt is based on a KEP method, kinetic energy is only slightly dissipated, supposedly as a result of the temporal integrator, given the very low Mach number of this test [Fig. 5(d)]; therefore, the lack of TEC translates into a lack of internal energy conservation by convection,

as displayed in Fig. 5(e) and theoretically expected. Finally, Fig. 5(f) reports the time evolution of global (normalized) entropy; although the scheme is not entropy preserving, it shows good entropy conservation properties, at least within the integration time explored in this work. The simulations were repeated at three different spatial resolutions, showing that the TEC property is asymptotically recovered at a rate $\mathcal{O}(h^2)$, in accordance with results of Section 4.1.2. Of note, the TEC error has again a dissipative character, i.e., it was not detrimental to the robustness of the simulation.

Finally, to examine the influence of the spurious oscillations on the flow field, a comparison between the KGP-Pt novel and KGP-Et current method is reported. Figure 6 shows the distribution of pressure and streamwise velocity comparing both approaches on a *coarse* mesh of 64×32 at an early stage of the flow evolution ($t/t_c = 0.2$); instants before the KGP-Et computation diverges. Due to lack of discrete pressure equilibrium, the existing KEP method (KGP-Et) produces a noisy pressure field, which also contaminates the velocity distribution [Figs. 6(a)-(c)]. Pressure oscillations are larger on the liquid-like region with respect to the ones arising in the gas-like region, close to the bottom boundary. This is in line with the spatial distribution of the pseudo-boiling line, which follows the roll-up KH structures and transports the oscillations closer to the top boundary. Of note, these results are qualitatively in line with those reported by Terashima and Koshi [14] for a transcritical jet. On the other hand, the newly proposed KEP+PEP method, KGP-Pt, is able to capture the pressure variations correctly, without the need of any artificial mechanism, and despite the limited number of points used to resolve the density gradient. This further underlines the importance of enforcing the PEP property for this class of problems, and demonstrates that: (i) the KEP property alone is not sufficient to tackle transcritical flows, and that (ii) the simultaneous enforcement of KEP and PEP provides stable and high-quality simulations without the need of any additional oscillation-suppressing mechanism.

Further insight is given in Fig. 7, where overshoots of pressure and density are clearly shown for the KGP-Et method compared to KGP-Pt. These are present both along a *horizontal* section [$y/L = 0.125$, Fig. 7(a)-(b)], as well as along the vertical centerline [$x/L = 0$, Fig. 7(c)-(d)]. In particular, the latter subset of figures highlights that the spurious oscillations become more severe near the top region, and the density field is clearly affected in the vertical direction. On the contrary, the KGP-Pt scheme provides smooth thermodynamic fields in either direction.

4.3. Direct numerical simulation of a transcritical channel flow

The DNS of a transcritical channel flow is finally computed utilizing the in-house flow solver RHEA [63] to demonstrate the applicability of the proposed KGP-Pt scheme in a complex turbulent case, and to compare it to KGP-Et. Despite the lack of the PEP property, the latter proved to be a stable scheme within high-pressure turbulent conditions at relatively low Reynolds numbers [60], and it is therefore used as a reference for comparison. For consistency, the configuration is similar to the mixing layer defined in Section 4.2: N_2 is used as operating fluid, whose critical pressure and temperature are $P_c = 3.4\,\mathrm{MPa}$ and $T_c = 126.2\,\mathrm{K}$, and its acentric factor is $\omega = 0.0372$. The system operates at a supercritical bulk pressure of $P_b/P_c = 2$ and confined between bottom (bw) and top (tw) isothermal walls, separated in this case at a distance $H = 2\delta$ with $\delta = 100\,\mu\mathrm{m}$ the channel half-height, at $T_{bw}/T_c = 0.75$ and $T_{tw}/T_c = 1.5$, respectively. This configuration forces the fluid to undergo a transcritical trajectory by operating within a thermodynamic region across the pseudo-boiling line. Following previous work [5], the friction Reynolds number selected at the bottom wall is $\mathrm{Re}_{\tau,bw} = \rho_{bw} u_{\tau,bw} \delta / \mu_{bw} = 100$ to ensure fully-developed turbulent flow conditions [4]. The corresponding dimensional parameters are: dynamic viscosity $\mu_{bw} = 1.6 \cdot 10^{-4}\,\mathrm{Pa \cdot s}$, density $\rho_{bw} = 839.4\,\mathrm{kg/m^3}$, and friction velocity $u_{\tau,bw} = 1.9 \cdot 10^{-1}\,\mathrm{m/s}$. The computational domain is $4\pi\delta \times 2\delta \times 4/3\pi\delta$ in the streamwise (x), wall-normal (y), and spanwise (z) directions, respectively. The grid is uniform in the streamwise and spanwise directions with resolutions in wall units (based on bw values) equal to $\Delta x^+ = 9.8$ and $\Delta z^+ = 3.3$, and stretched toward the walls in the vertical direction with the first grid point at $y^+ = y u_{\tau,bw}/\nu_{bw} = 0.1$ and with sizes in the range $0.4 \lesssim \Delta y^+ \lesssim 2.3$. Thus, this arrangement corresponds to a grid size of $128 \times 128 \times 128$ points. Based on the estimates provided by Jofre and Urzay [1], the characteristic length scale for density gradients in this case is approximately $10\times$ larger than the Kolmogorov scale, therefore the latter is the driving factor to select mesh resolution. The selected grid size is thus assumed to resolve all the relevant

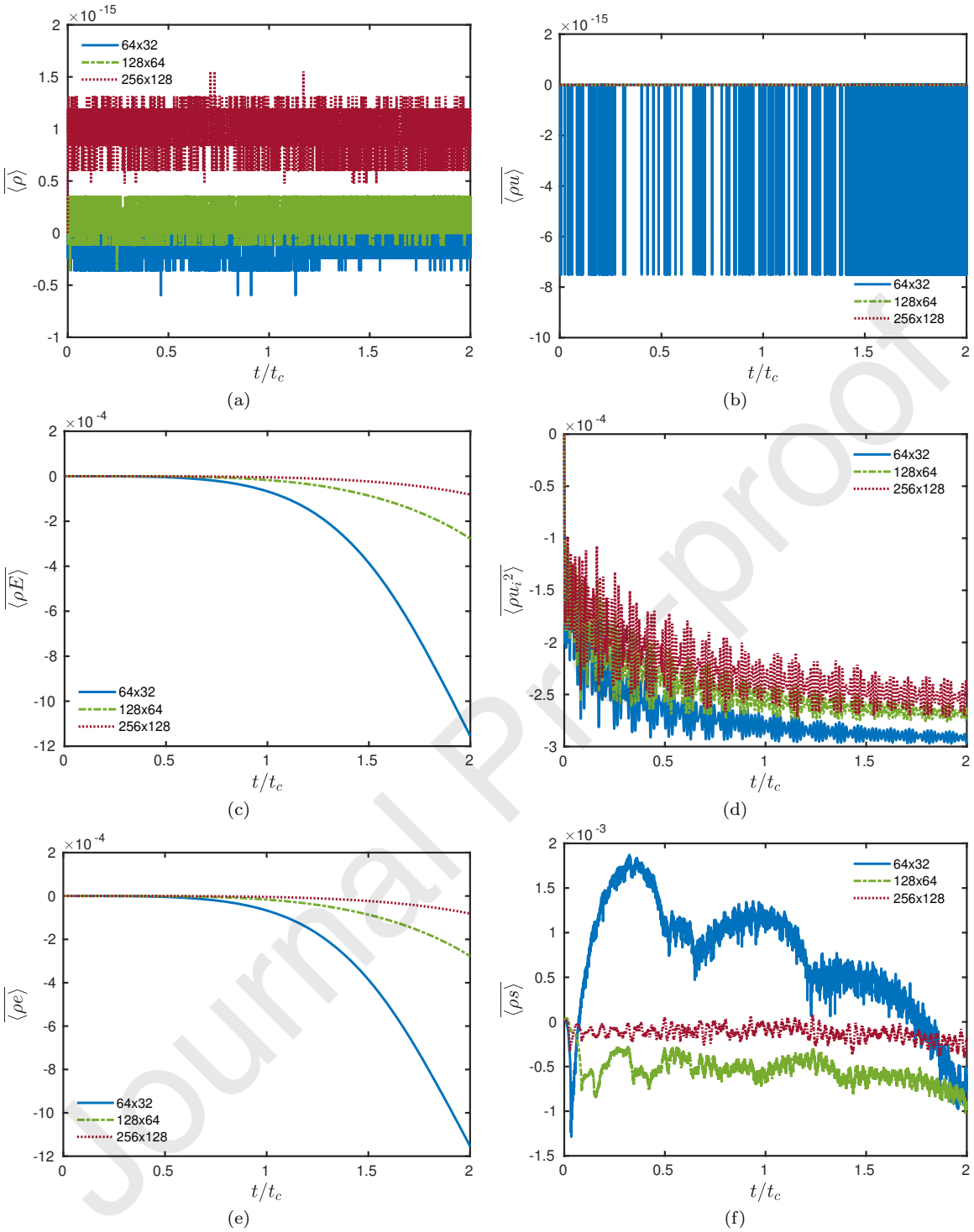

Figure 5: Temporal evolution of several quantities for the 2D inviscid mixing, for 64×32 (solid-blue), 128×64 (dashed-green) and 256×128 (dotted-red) mesh size for (a) ρ, (b) ρu, (c) ρE, (d) $\rho {u_i}^2$, (e) ρe and (f) ρs normalized according to Eq. (32). Scheme used: KGP-Pt.

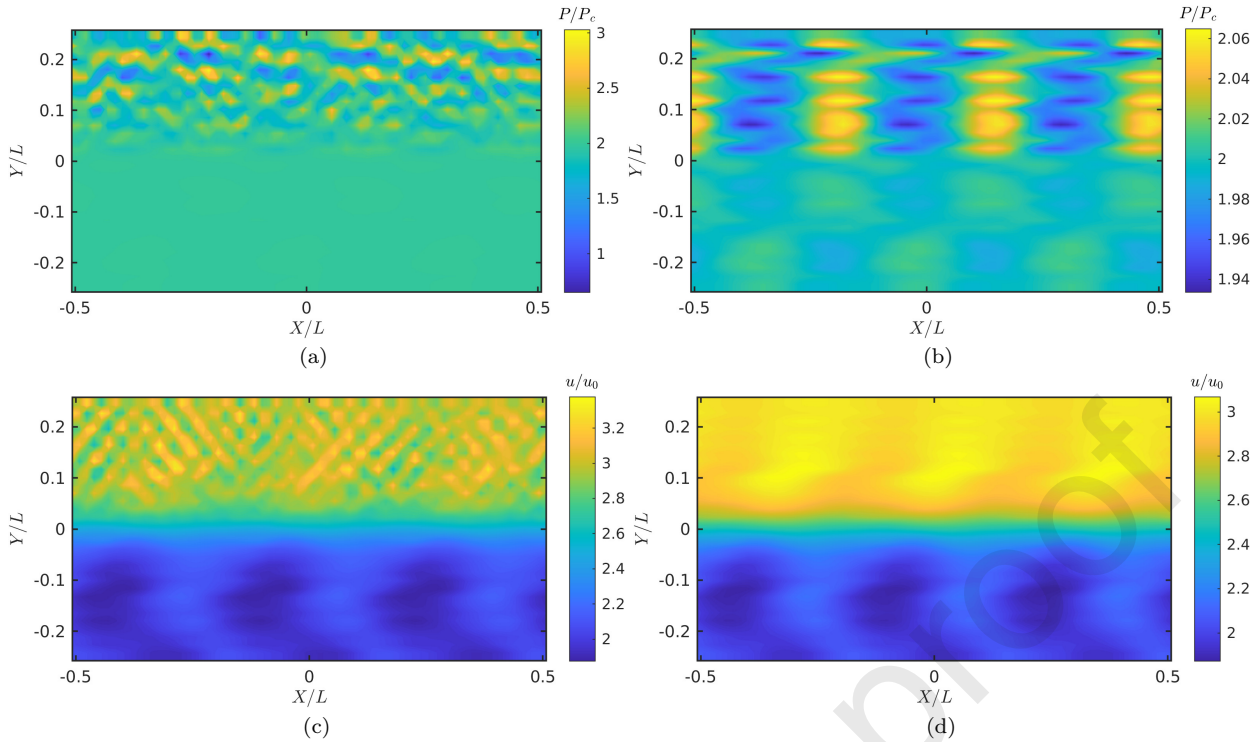

Figure 6: 2D inviscid mixing layer in a transcritical regime. Contours at $t/t_c = 0.2$ for 64×32 mesh size with CFL $= 0.3$ comparing the KGP-Et (a,c) and the KGP-Pt (b,d) schemes for normalized (a,b) pressure (with respect to the critical point) and (c,d) streamwise velocity (with respect to $\delta u = 10m/s$).

flow scales as it is finer than any of the resolutions used in the DNS by Lee and Moser [64], and $2\times$ finer in each direction with respect to Chevalier et al. [65]. The simulation strategy starts from a linear velocity profile with random fluctuations [66], which is advanced in time to reach turbulent steady-state conditions after approximately five flow-through-time (FTT) units; based on the bulk velocity u_b and the length of the channel $L_x = 4\pi\delta$, a FTT is defined as $t_b = L_x/u_b \sim \delta/u_\tau$. In this regard, flow statistics are collected for roughly 10 FTTs once steady-state conditions are achieved.

Figure 8 presents a comparison in terms of non-dimensional first-order statistics; in particular, Fig. 8(a) shows that there are no significant differences between the two numerical schemes in terms of mean streamwise velocity in wall units. Similarly, Fig. 8(b) depicts the time-averaged temperature in viscous units $T^+ = (T - T_w)/T_\tau$, with T_w the wall temperature and $T_\tau = [\kappa/(\rho c_P u_\tau)(d\langle T\rangle/dy)]$, and no visible differences are displayed. Similar conclusions can be drawn for the Favre-averaged fluctuations reported in Fig. 9 for (a) bottom wall and (b) top wall. The profiles of the two schemes match to plotting accuracy, which reliably confirms the applicability and robustness of the novel scheme in the context of transcritical 3D applications. For completeness, Favre-averaged fluctuations for temperature are shown in Fig. 10(a) for bottom and walls, while the Prandtl number $Pr = c_p\mu/\kappa$ and the compressibility factor $Z = P/(R_u\rho T)$ are reported in Fig. 10(b). The analysis again confirms that the novel scheme KGP-Pt does not induce any drift in terms of momentum and thermal diffusivity, and that non-ideal gas effects are well captured.

5. Conclusions

This work has focused on the derivation and analysis of kinetic-energy-preserving (KEP) and pressure-equilibrium-preserving (PEP) numerical schemes for the computation of discontinuity-free compressible flows governed by a general real-gas equation of state. The underlying premise is that these two properties are especially crucial for high-fidelity scale-resolving simulations of turbulent flows in the trans- and supercritical

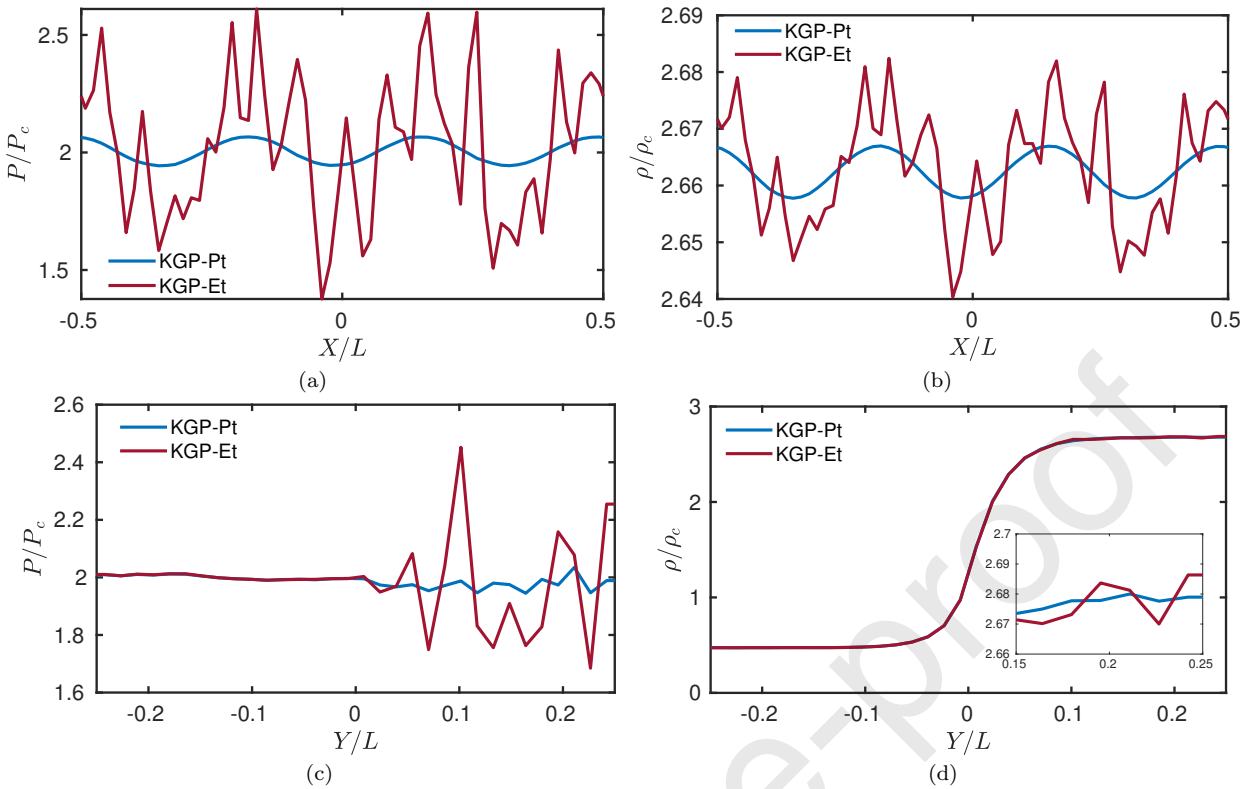

Figure 7: Comparison of KGP-Pt and KGP-Et for the 2D mixing layer in a transcritical regime at $t/t_c = 0.2$, with a 64×32 mesh and CFL $= 0.3$. Plots of normalized (a,c) pressure and (b,d) density with respect to critical point at (a,b) $y/L_y = 0.125$ along horizontal direction and at (c,d) $x/L_x = 0$ along vertical direction.

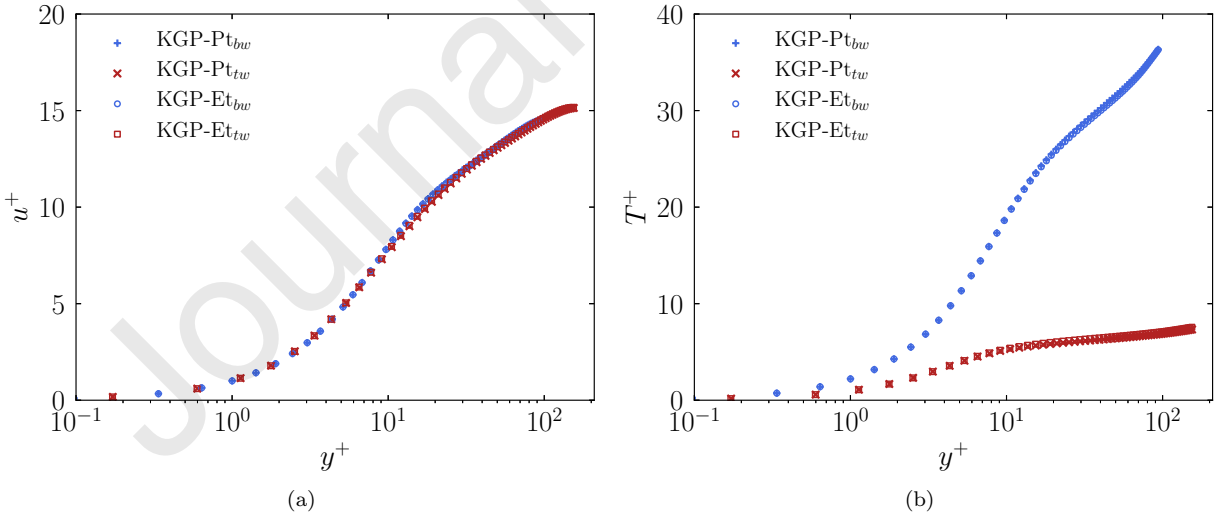

Figure 8: Time-averaged first-order statistics comparison of (a) streamwise velocity u^+, and (b) temperature T^+ along the wall-normal direction y^+ at the bottom (bw) and top (tw) walls for KGP-Pt and KGP-Et cases.

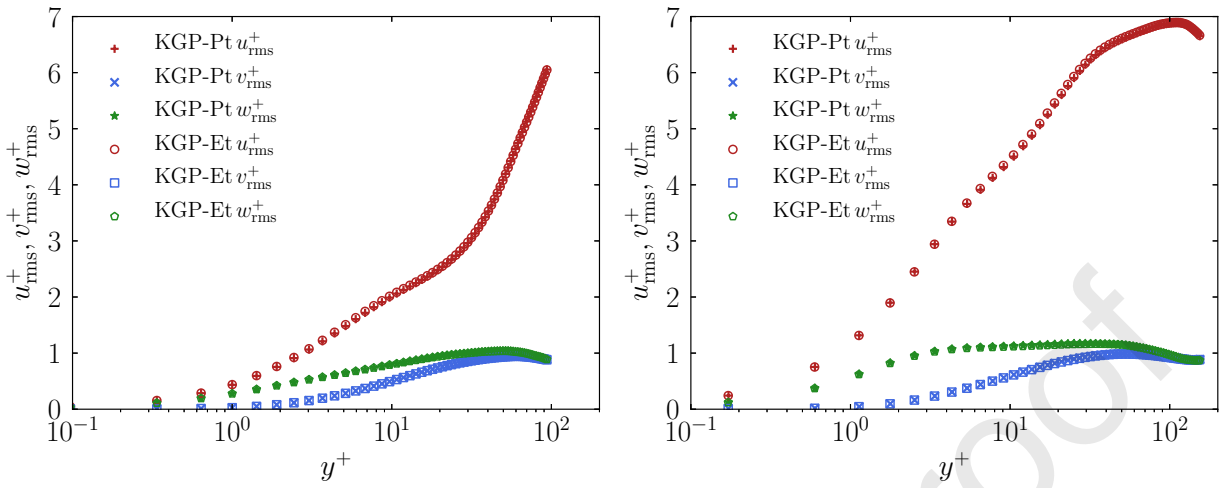

Figure 9: Favre-averaged fluctuations of u^+, v^+ and w^+ along the wall-normal direction y^+ at (a) the bottom (bw) and (b) top (tw) walls for KGP-Pt and KGP-Et.

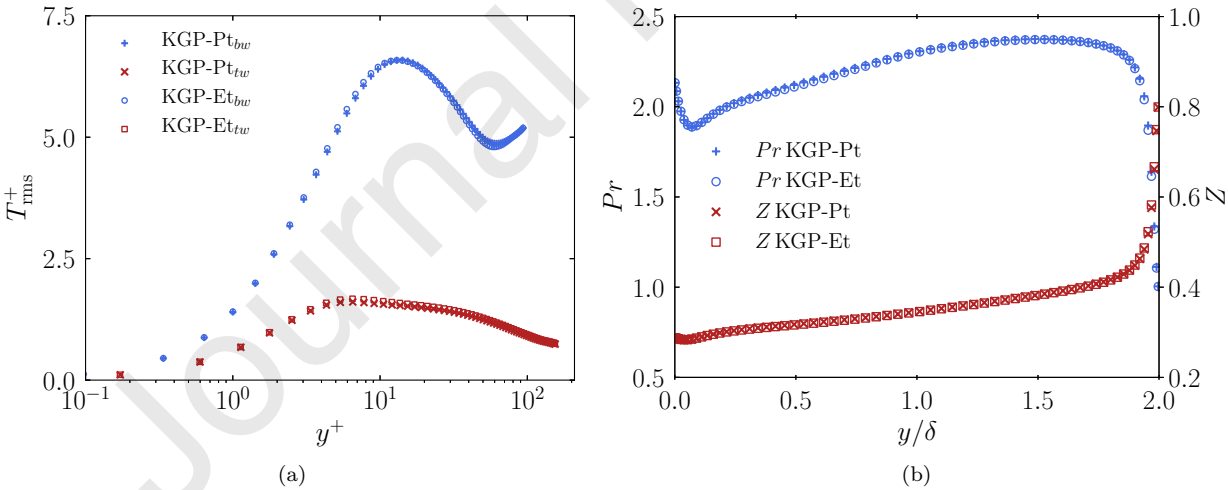

Figure 10: (a) Favre-averaged fluctuations of T^+ along y^+ at the bottom (bw) and top (tw) walls, and (b) Prandtl number Pr and compressibility factor Z along the wall-normal direction normalized by channel half-height y/δ for KGP-Pt and KGP-Et.

thermodynamic regimes. Previous works have struggled to tackle this class of fluid flows, which is relevant in many engineering applications; so far, the practical solution has relied on stabilized discretization methods, at the expense of the simulation fidelity. In this work, it is conjectured that the simultaneous enforcement of the KEP and PEP properties at the discrete level can lead to stable, dissipation-free and physically-compatible simulations of transcritical turbulent flows, even on relatively coarse grids.

A rigorous framework for the derivation and analysis of KEP/PEP methods has been introduced. While the enforcement of the KEP property is directly inherited from the results previously obtained for ideal-gas flows, the derivation of PEP schemes (i.e., discretizations capable of maintaining constant pressure when both pressure and velocity are initially uniform) is far from trivial in the case of general, non-linear equations of state of type $P = P(\rho, e)$. When total or internal energy are directly discretized along with mass and momentum, a novel class of schemes –named CR– has been derived. For these methods, the use of a discrete product rule is not necessary to demonstrate the discrete enforcement of PEP. However, it is found that the discrete satisfaction of the chain rule by the spatial differential operator is still needed and constitutes a *barrier* for the derivation of PEP schemes based on the evolution of total or internal energy, regardless of the split forms selected. Classical second-order centered schemes are indeed known to satisfy a modified chain rule that is only accurate to second order. A novel class of schemes based on the solution of an evolution equation for pressure has thus been introduced. One of the methods of this class, labeled KGP-Pt, is PEP and globally and locally preserves mass, momentum and kinetic energy. On the other hand, total energy conservation (TEC) is sacrificed, as both the chain and the product rules need to be invoked at the discrete level to satisfy TEC, again regardless of the split form utilized for the non-linear terms.

The novel schemes have been numerically assessed in a series of tests of increasing complexity, and compared to several existing methods commonly utilized for compressible flows and/or tailored for trans-/supercritical turbulence. In a one-dimensional advection test of a density wave, the only schemes that were able to maintain the pressure equilibrium in a real-gas framework were the novel KGP-Pt and a stabilized pressure-based formulation with convective terms expressed in divergence form, and with compact filtering applied to the conservative variables. However, the latter scheme is inherently dissipative in nature. Similarly, other strategies specifically developed for this class of problems, like the double-flux scheme, required numerical dissipation to remain stable and free of pressure oscillations. An asymptotic analysis of the errors revealed that the total energy conservation error of the KGP-Pt has a slightly dissipative character and scales as $\mathcal{O}(h^2)$, as predicted by the theoretical framework; on the other hand, methods of the CR class did not show any significant practical advantage over other non-PEP schemes. A subsequent two-dimensional test (transcritical mixing layer) further emphasized the importance of enforcing the PEP property: a reference state-of-the-art KEP scheme based on total energy, labeled KGP-Et, generated significant pressure disturbances at the pseudo-interface, while KGP-Pt provided smooth flow fields and stable integration for this challenging inviscid test, even on coarse grids, and without the need of any stabilization mechanism, while only slightly dissipating internal energy. Finally, the applicability of the KGP-Pt was demonstrated for the direct numerical simulation of a transcritical channel flow. For this case, pressure oscillations are mitigated by physical viscosity and standard KEP schemes can be profitably applied. The lack of TEC of the novel scheme did not cause any deviation for first- and second-order statistics, as well as for other thermodynamic quantities, when compared to KGP-Et.

In summary, based on the analysis presented in this paper, the development of methods that are total energy conservative, and simultaneously KEP and PEP, appears to be hampered by the lack of a discrete chain rule for linear finite-differencing schemes, in the case of real-gas equations of state. This problem is analogous to the long-standing issue of entropy conservation by finite-difference or finite-volume schemes based on arithmetic averages of flow variables, i.e., based on the split forms presented in this paper. More in general, this issue is relevant for any invariant quantity that is related to primary variables through non-linear, non-algebraic relationships. A potential solution to overcome the above-mentioned *barrier* is to formulate the discretization directly in a finite-volume framework, and select proper non-linear averages for the construction of the numerical fluxes. This option was not considered in this study and could be the subject of future work. For real-gas equations of state such as the Peng-Robinson one, however, this process is anticipated to be quite cumbersome due to its highly non-linear character; some sort of "compromise" (e.g., local linearization) is therefore expected in any case.

In the specific context of trans-/supercritical fluids turbulence, the newly proposed KGP-Pt scheme appears to be a suitable candidate for stable high-fidelity scale-resolving simulations, and has shown superior behaviour compared to existing KEP-only methods, as well as to previous methods tailored for this thermodynamic regime. In the results reported in the paper, the lack of TEC was not detrimental to the results, whereas enforcing the PEP property was of utmost importance in guaranteeing solution fidelity and stability. Nonetheless, care should be taken in terms of generalizing this conclusion, especially when considering different flow regimes; further analyses are warranted in this regard. Generally speaking, the relative importance of the various (primary and secondary) conservation properties appears to be strongly associated with the physics of the problem under study. While enforcing as many conservation properties as possible is certainly beneficial, sacrificing some over others according to the specific flow regime might be a necessary compromise to obtain stable and physically relevant solutions, especially if "fully-conservative" approaches are challenging to obtain or costly to implement/use.

Future work should focus on (i) further characterizing the properties and numerical behaviour of the proposed class of schemes at higher Reynolds and Mach numbers, and (ii) seeking the simultaneous enforcement of KEP, TEC, PEP and potentially entropy conservation based on non-linear fluxes in the context of thermally-perfect and real-gas thermodynamics.

Acknowledgements

The authors gratefully acknowledge the *Formació de Professorat Universitari* scholarship (FPU-UPC R.D 103/2019) of the Universitat Politècnica de Catalunya · BarcelonaTech (UPC) (Spain), the *Serra Húnter* and SRG (2021-SGR-01045) programs of the Generalitat de Catalunya (Spain), the *Beatriz Galindo* program (Distinguished Researcher, BGP18/00026) of the Ministerio de Educación y Formación Profesional (Spain), and the computer resources at FinisTerrae III & MareNostrum and the technical support provided by CESGA & Barcelona Supercomputing Center (RES-IM-2023-1-0005, RES-IM-2023-2-0005). The authors are thankful to G. Coppola for insightful discussions on a preliminary draft of the discretization framework.

Funding sources

This work is funded by the European Union (ERC, SCRAMBLE, 101040379). Views and opinions expressed are however those of the authors only and do not necessarily reflect those of the European Union or the European Research Council. Neither the European Union nor the granting authority can be held responsible for them.

Data availability and reproducibility

The data reported in this paper was produced by in-house software that is available open-source.

A MATLAB code, labeled as High-Pressure Compressible Flow Solver (HPCFS), was used to obtain part of the numerical results presented in this work. It can be accessed at: `https://github.com/marc-bernades/HPCFS`. HPCFS was designed to serve as a flexible tool to develop methods, numerical schemes and design new cases and approaches, and includes both ideal-gas and real-gas thermodynamic frameworks. The code is equipped with several comments for readability. Additionally, the repository includes (i) a description of the code, (ii) instructions and a guide for users and (iii) validation reports. The numerical tests presented in Sections 4.1 and 4.2 (1D advective wave and 2D mixing layer) can be fully reproduced by the interested reader. Other canonical tests are also available (e.g., Taylor-Green vortex, vortex advection, high-pressure thermodynamic analysis, lid-driven cavity and channel flow).

The open-source Reproducible Hybrid-architecture flow solver Engineered for Academia (RHEA) [63] can be accessed at: `https://gitlab.com/ProjectRHEA/flowsolverrhea`. RHEA is written in C++, using object-oriented programming, utilizes YAML and HDF5 for input/output operations, and targets hybrid supercomputing architectures. RHEA was utilized to obtain the transcritical 3D channel flow results presented in Section 4.3. The test is also available in the repository and can be reproduced by the user.

References

[1] L. Jofre, J. Urzay, A characteristic length scale for density gradients in supercritical monocomponent flows near pseudoboiling, Annual Research Briefs, Center for Turbulence Research, Stanford University (2020) 277–282.

[2] L. Jofre, J. Urzay, Transcritical diffuse-interface hydrodynamics of propellants in high-pressure combustors of chemical propulsion systems, Prog. Energy Combust. Sci. 82 (2021) 100877.

[3] M. Bernades, F. Capuano, L. Jofre, Flow physics characterization of microconfined high-pressure transcritical turbulence, Proceedings of the Summer Program 2022, Center for Turbulence Research, Stanford University (2022) 215–224.

[4] M. Bernades, L. Jofre, Thermophysical analysis of microconfined turbulent flow regimes at supercritical fluid conditions in heat transfer applications, J. Heat Transfer 144 (2022) 082501.

[5] M. Bernades, F. Capuano, L. Jofre, Microconfined high-pressure transcritical fluid turbulence, Phys. Fluids 35 (2023) 015163.

[6] L. Jofre, M. Bernades, F. Capuano, Dimensionality reduction of non-buoyant microconfined high-pressure transcritical fluid turbulence, Int. J. Heat Fluid Flow 102 (2023) 109169.

[7] G. Coppola, F. Capuano, L. de Luca, Discrete energy-conservation properties in the numerical simulation of the navier–stokes equations, Appl. Mech. Rev. 71 (2019).

[8] A. M. Dunton, L. Jofre, G. Iaccarino, A. Doostan, Pass-efficient methods for compression of high-dimensional turbulent flow data, J. Comput. Phys. 423 (2020) 109704.

[9] R. Abgrall, How to prevent pressure oscillations in multicomponent flow calculations: A quasi conservative approach, J. Comput. Phys. 125 (1996) 150–160.

[10] N. Shima, Y. Kuya, Y. Tamaki, S. Kawai, Preventing spurious pressure oscillations in split convective form discretization for compressible flows, J. Comput. Phys. 427 (2021) 110060.

[11] T. Schmitt, L. Selle, A. Ruiz, B. Cuenot, Large-eddy simulation of supercritical-pressure round jets, AIAA journal 48 (2010) 2133–2144.

[12] R. Abgrall, S. Karni, Computations of compressible multifluids, J. Comput. Phys. 169 (2000) 594–623.

[13] P. C. Ma, Y. Lv, M. Ihme, An entropy-stable hybrid scheme for simulations of transcritical real-fluid flows, J. Comput. Phys. 340 (2017) 330–357.

[14] H. Terashima, M. Koshi, Approach for simulating gas-liquid-like flows under supercritical pressures using a high-order central differencing scheme, J. Comput. Phys. 231 (2012) 6907–6923.

[15] S. Kawai, H. Terashima, H. Negishi, A robust and accurate numerical method for transcritical turbulent flows at supercritical pressure with an arbitrary equation of state, J. Comput. Phys. 300 (2015) 116–135.

[16] G. Lacaze, T. Schmitt, A. Ruiz, J. Oefelein, Comparison of energy-,pressure- and enthalpy-based approaches for modeling supercritical flows, Computers & Fluids 181 (2019) 35–56.

[17] M. R. Visbal, D. V. Gaitonde, On the use of higher-order finite-difference schemes on curvilinear and deforming meshes, J. Comput. Phys. 181 (2002) 155–185.

[18] F. Toro, Riemann solvers and numerical methods for fluid dynamics, Springer (USA), 3rd edition, 2009.

[19] C. Shu, High order ENO and WENO schemes for computational fluid dynamics, Lecture Notes in Computational Science and Engineering 9 (1999) 439–582.

[20] W. Feiereisen, W. Reynolds, J. Ferziger, Numerical simulation of a compressible, homogeneous, turbulent shear flow. report tf-13, thermosciences division, Mechanical Engineering, Stanford University (1981) 759.

[21] C. A. Kennedy, A. Gruber, Reduced aliasing formulations of the convective terms within the navier–stokes equations for a compressible fluid, J. Comput. Phys. 227 (2008) 1676–1700.

[22] S. Pirozzoli, Generalized conservative approximations of split convective derivative operators, Journal of Computational Physics 229 (2010) 7180–7190.

[23] G. Coppola, F. Capuano, S. Pirozzoli, L. de Luca, Numerically stable formulations of convective terms for turbulent compressible flows, J. Comput. Phys. 382 (2019) 86–104.

[24] Y. Kuya, K. Totani, S. Kawai, Kinetic energy and entropy preserving schemes for compressible flows by split convective forms, Journal of Computational Physics 375 (2018) 823–853.

[25] Y. Tamaki, Y. Kuya, S. Kawai, Comprehensive analysis of entropy conservation property of non-dissipative schemes for compressible flows: KEEP scheme redefined, Journal of Computational Physics 468 (2022) 111494.

[26] P. K. Subbareddy, G. V. Candler, A fully discrete, kinetic energy consistent finite-volume scheme for compressible flows, Journal of Computational Physics 228 (2009) 1347–1364.

[27] Y. Morinishi, Skew-symmetric form of convective terms and fully conservative finite difference schemes for variable density low-mach number flows, Journal of Computational Physics 229 (2010) 276–300.

[28] W. Rozema, J. Kok, R. Verstappen, A. Veldman, A symmetry-preserving discretisation and regularisation model for compressible flow with application to turbulent channel flow, Journal of Turbulence 15 (2014) 386–410.

[29] A. K. Edoh, A new kinetic-energy-preserving method based on the convective rotational form, Journal of Computational Physics 454 (2022) 110971.

[30] H. Ranocha, G. J. Gassner, Preventing pressure oscillations does not fix local linear stability issues of entropy-based split-form high-order schemes, Communications on Applied Mathematics and Computation (2021) 1–24.

[31] S. S. Jain, P. Moin, A kinetic energy–and entropy-preserving scheme for compressible two-phase flows, J. Comput. Phys. 464 (2022) 111307.

[32] Y. Fujiwara, Y. Tamaki, S. Kawai, Fully conservative and pressure-equilibrium preserving scheme for compressible multicomponent flows, Journal of Computational Physics 478 (2023) 111973.

[33] D. Y. Peng, D. B. Robinson, A new two-constant equation of state, Ind. Eng. Chem. Fundam. 15 (1976) 59–64.

[34] A. Burcat, B. Ruscic, Third millennium ideal gas and condensed phase thermochemical database for combustion with updates from active thermochemical tables, Technical Report, Argonne National Laboratory, 2005.

[35] T. H. Chung, L. L. Lee, K. E. Starling, Applications of kinetic gas theories and multiparameter correlation for prediction of dilute gas viscosity and thermal conductivity, Ind. Eng. Chem. Fund. 23 (1984) 8–13.

[36] T. H. Chung, M. Ajlan, L. L. Lee, K. E. Starling, Generalized multiparameter correlation for nonpolar and polar fluid transport properties, Ind. Eng. Chem. Fund. 27 (1988) 671–679.

[37] B. E. Poling, J. M. Prausnitz, J. P. O'Connell, Properties of Gases and Liquids, McGraw Hill, New York (USA), 5th edition, 2001.

[38] G. Coppola, A. E. Veldman, Global and local conservation of mass, momentum and kinetic energy in the simulation of compressible flow, Journal of Computational Physics 475 (2023) 111879.

[39] F. Capuano, G. Coppola, L. Rández, L. de Luca, Explicit Runge–Kutta schemes for incompressible flow with improved energy-conservation properties, J. Comput. Phys. 328 (2017) 86–94.

[40] E. Tadmor, Entropy stability theory for difference approximations of nonlinear conservation laws and related time-dependent problems, Acta Numerica 12 (2003) 451–512.

[41] H. Ranocha, Comparison of some entropy conservative numerical fluxes for the euler equations, Journal of Scientific Computing 76 (2018) 216–242.

[42] A. R. Winters, C. Czernik, M. B. Schily, G. J. Gassner, Entropy stable numerical approximations for the isothermal and polytropic Euler equations, BIT Numerical Mathematics 60 (2020) 791–824.

[43] M. C. Hansen, T. A. Fisher, Entropy Stable Discretization of Compressible Flows in Thermochemical Nonequilibrium, Technical Report, Sandia National Lab.(SNL-NM), Albuquerque, NM (United States), 2019.

[44] A. Gouasmi, K. Duraisamy, S. M. Murman, Formulation of entropy-stable schemes for the multicomponent compressible euler equations, Comput Methods Appl Mech Eng. 363 (2020) 112912.

[45] A. Peyvan, K. Shukla, J. Chan, G. Karniadakis, High-order methods for hypersonic flows with strong shocks and real chemistry, arXiv preprint arXiv:2211.12635 (2022).

[46] E. J. Ching, R. F. Johnson, A. D. Kercher, Positivity-preserving and entropy-bounded discontinuous galerkin method for the chemically reacting, compressible euler equations. part i: The one-dimensional case, arXiv preprint arXiv:2211.16254 (2022).

[47] A. E. P. Veldman, Supraconservative finite-volume methods for the euler equations of subsonic compressible flow, SIAM Review 63 (2021) 756–779.

[48] A. Jameson, The construction of discretely conservative finite volume schemes that also globally conserve energy or entropy, Journal of Scientific Computing 34 (2008) 152–187.

[49] C. De Michele, G. Coppola, Numerical treatment of the energy equation in compressible flows simulations, Computers & Fluids (2022) 105709.

[50] A. E. Honein, P. Moin, Higher entropy conservation and numerical stability of compressible turbulence simulations, Journal of Computational Physics 201 (2004) 531–545.

[51] H. Ranocha, Mimetic properties of difference operators: product and chain rules as for functions of bounded variation and entropy stability of second derivatives, BIT Numerical Mathematics 59 (2019) 547–563.

[52] C. De Michele, G. Coppola, Numerical treatment of the energy equation in compressible flows simulations, Computers & Fluids 250 (2023) 105709.

[53] A. Jameson, Formulation of kinetic energy preserving conservative schemes for gas dynamics and direct numerical simulation of one-dimensional viscous compressible flow in a shock tube using entropy and kinetic energy preserving schemes, Journal of Scientific Computing 34 (2008) 188–208.

[54] S. K. Lele, Compact finite difference schemes with spectral-like resolution, Journal of computational physics 103 (1992) 16–42.

[55] F. Capuano, A. Mastellone, E. D. Angelis, A conservative overlap method for multi-block parallelization of compact finite-volume schemes, Computers & Fluids 159 (2017) 327–337.

[56] N. A. Okong'o, J. Bellan, Direct numerical simulation of a transitional supercritical binary mixing layer: heptane and nitrogen, Journal of Fluid Mechanics 464 (2002) 1–34.

[57] A. K. Edoh, N. L. Mundis, C. L. Merkle, A. R. Karagozian, V. Sankaran, Comparison of artificial-dissipation and solution-filtering stabilization schemes for time-accurate simulations, Journal of Computational Physics 375 (2018) 1424–1450.

[58] E. Lamballais, R. V. Cruz, R. Perrin, Viscous and hyperviscous filtering for direct and large-eddy simulation, Journal of Computational Physics 431 (2021) 110115.

[59] E. F. Toro, M. Spruce, W. Speares, Restoration of the contact surface in the hll-riemann solver, Shock Waves 4 (1994) 25–34.

[60] M. Bernades, L. Jofre, F. Capuano, Investigation of a novel numerical scheme for high-pressure supercritical fluids turbulence, Proceedings of the Summer Program 2022, Center for Turbulence Research, Stanford University (2022) 225–234.

[61] F. Ducros, V. Ferrand, F. Nicoud, C. Weber, D. Darracq, C. Gacherieu, T. Poinsot, Large-eddy simulation of the shock/turbulence interaction, J. Comput. Phys. 1252 (1999) 517–549.

[62] N. Sharan, G. Matheou, P. Dimotakis, Turbulent shear-layer mixing: initial conditions, and direct-numerical and large-eddy simulations, J. Fluid Mech. 877 (2019) 35–81.

[63] L. Jofre, A. Abdellatif, G. Oyarzun, RHEA - an open-source Reproducible Hybrid-architecture flow solver Engineered for Academia, J. Open Source Softw. 8 (2023) 4637.

[64] M. Lee, R. D. Moser, Direct numerical simulation of turbulent channel flow up to $Re_\tau \approx 5200$, J. Fluid. Mech. 774 (2015) 395–415.

[65] M. Chevalier, J. Hœpffner, T. R. Bewley, D. S. Henningson, State estimation in wall-bounded flow systems. part 2. turbulent flows, J. Fluid Mech. 552 (2006) 167–187.
[66] K. S. Nelson, O. B. Fringer, Reducing spin-up time for simulations of turbulent channel flow, Phys. Fluids 29 (2017) 105101.

Declaration of interests

☐ The authors declare that they have no known competing financial interests or personal relationships that could have appeared to influence the work reported in this paper.

☒ The authors declare the following financial interests/personal relationships which may be considered as potential competing interests:

Lluis Jofre reports financial support was provided by European Research Council.

Marc Bernades: Conceptualization; Methodology; Software; Validation; Formal analysis; Investigation; Writing - Original Draft
Lluis Jofre: Conceptualization; Software; Writing - Review & Editing; Supervision; Funding acquisition
Francesco Capuano: Conceptualization; Methodology; Formal analysis; Writing - Review & Editing; Supervision